Materials Advances

ROYAL SOCIETY OF CHEMISTRY

REVIEW

View Article Online
View Journal | View Issue

Cite this: *Mater. Adv.*, 2021, **2**, 1229

Cu(II/I) redox couples: potential alternatives to traditional electrolytes for dye-sensitized solar cells†

K. S. Srivishnu,[ab] Seelam Prasanthkumar [ab] and Lingamallu Giribabu *[ab]

Received 29th December 2020,
Accepted 20th January 2021

DOI: 10.1039/d0ma01023e

rsc.li/materials-advances

The redox shuttle is one of the essential ingredients in dye-sensitized solar cell devices. Though the I^-/I_3^- redox couple has dominated in the last couple of decades, however, due to the loss of open-circuit potential, complementary absorption with a sensitizer and the volatile nature restricts the module development. Metal complexes with variable oxidation states are probable alternative candidates as redox shuttles due to the change in their redox potentials with varying ligands in order to suit different sensitizers. Co(III/II) redox couples using polypyridyl ligands have been widely used in DSSC and have crossed the device efficiency of 14%. However, mass transport constraints and health hazards exist due to the commercialization of technology. Inspired from biological electron transfer reactions, Cu(II/I) redox shuttles have gained much attention as redox couples for DSSC applications in recent years. Particularly in low light conditions, it minimizes mass transport, has a device efficiency greater than 32%, and has potential in Internet of Things (IoT) applications. In this review, recent advancements in the use of Cu(II/I) redox shuttles using polypyridyl ligands for DSSC applications are presented.

1. Introduction

As a consequence of profusely increasing global energy demands and environmental concerns, dye-sensitized solar cells (DSSCs) are becoming an alternative to existing photovoltaic technologies.[1–5] However, both first (silicon photovoltaic technologies) and second-generation solar cells (thin film solar cells such as CdTe and GaAs) have their own limitations in

[a] *Polymers & Functional Materials Division, CSIR-Indian Institute of Chemical Technology (IICT), Tarnaka, 500007, Telangana, India. E-mail: giribabu@iict.res.in*
[b] *Academy of Scientific and Innovative Reseaerch (AcSIR), Ghaziabad 201002, India*

† Electronic Supplementary Information (ESI) available. See DOI: 10.1039/d0ma01023e

K. S. Srivishnu

Srivishnu K. S. obtained an MSc (Chemistry) from Osmania University, Telangana, India, in 2018. Subsequently, he obtained the DST-Inspire fellowship and joined as a junior research fellow in Dr L. Giribabu's group at Polymers & Functional Materials Division, CSIR-Indian Institute of Chemical technology (IICT), India. His research interest is focused on the design of redox couples and hole transport materials for dye-sensitized/perovskite solar cells applications.

Seelam Prasanthkumar

Seelam Prasanthkumar received his PhD degree in organic chemistry from CSIR-National Institute of Interdisciplinary Science and Technology (NIIST), Trivandrum, India in 2012. Afterwards, he joined as a post-doctoral fellow in the group of Prof. Dr Takuzo Aida, RIKEN, Japan. He is currently working as a DST-Inspire faculty at Inorganic & Physical Chemistry Division, CSIR-Indian Institute of Chemical technology (IICT), Hyderabad, India. His research interest includes developing novel materials for organic and perovskite solar cell devices.

aspects such as purity requirement, cost, scarcity, and toxicity of the required materials. For this reason, excitonic solar cells have been established to as a dominant energy alternative to photovoltaic technologies, where excitonic devices belong to third-generation solar cells. Among third-generation solar cells, DSSCs are most important devices being on the verge of commercialization.[6] The priority of DSSCs over other conventional solar cells is primarily due to their advantages such as cost effectiveness, easy fabrication, reduced environmental hazards, and good temperature performance over other photovoltaic technologies. Moreover, low-light performance can be achieved through DSSCs, which is not possible in conventional silicon solar cells.[7] The hypothesis of DSSCs was first accomplished by Grätzel and co-workers in 1991 with a device efficiency of 7.1% using the Ru(II)-polypyridyl complex as the sensitizer and I^-/I_3^- as the redox mediator.[8] Since then number of academicians and industries have paid attention to improve the certified device efficiency up to 11.9% and the device efficiency up to 14.3%.[9–11] The enhanced device efficiency has been made possible through the re-designing of various components of the device, which includes the photoanode, transparent conducting substrate, sensitizer, redox electrolyte, counter electrode, and also by adopting new fabrication techniques. Among all these components of the device, the redox electrolyte acts as a pivotal component in attaining high efficiency and durability of the device.[12,13]

The electrolyte is the most critical component of the device as it is accountable for inner charge carrier transport between electrodes and continuously restores the dye and itself during the DSSC process.[14–17] Three parameters by which the power conversion efficiency (PCE) is determined in DSSCs are photocurrent density (J_{SC}), photovoltage (V_{OC}), and fill factor (ff). The electrolyte plays an important role in all three parameters.

Lingamallu Giribabu

Lingamallu Giribabu received his PhD degree in chemistry from the University of Hyderabad in 2000. Before joining CSIR-Indian Institute of Chemical technology (IICT), Hyderabad, India, as a Scientist in 2003, he worked with Dr Martin R. Johnston (Central Queensland University, Australia) and Prof. Karl M. Kadish (University of Houston, Houston, USA) as a postdoctoral fellow. He has been working as a Senior Principal Scientist at the Indian Institute of Chemical Technology, India, since 2018. His research interests include the development of low-cost new efficient materials for dye-sensitized solar cells, donor–acceptor systems, non-linear optical properties, and the photoelectrochemistry of tetrapyrrolic compounds. He has published over 200 research articles, patents, review articles, and a couple of book chapters.

The transport of redox couple components can affect the photocurrent density of the charge carrier in the electrolyte and can affect the fill factor; more importantly, the redox potential of the electrolyte can drastically affect the photovoltage. Considering all these points, the electrolyte should be optimized in view of the device efficiency and durability. DSSCs have been used with the redox couple I^-/I_3^- in the volatile acetonitrile solvent.[18–20] The liquid electrolyte was used for many years before the emergence of new electrolytes and in many cases, even in the present scenario, it is still being used. The iodide redox couple has its own disadvantages such as reduced long-term stability, performance control, and incompatibility with several metal compounds.[15] The redox shuttle shows a slight loss in the open circuit voltage (V_{OC}) and a significant loss in the short circuit current density (J_{SC}). Due to complimentary absorption in the visible region with sensitizers, the redox shuttle I^-/I_3^- leads to photocurrent loss. Moreover, iodine can also be used as an oxidizing agent; however, it corrodes precious noble metals used in device fabrication such as platinum and silver. Therefore, it is necessary to investigate alternative redox couples keeping the technical drawbacks of I^-/I_3^- redox couple in mind and also the large scale mini-module production of DSSC devices for commercialization.

A great variety of redox couples have been used in DSSCs, including inorganic redox couples for instance Br^-/Br_3^-, $SeCN^-/(SeCN)_2$, $SCN^-/(SCN)_2$, and S^{2-}/S, which is also known as sulphide/polysulfide (S^{2-}/S_n^{2-}).[21–26] All these inorganic redox couples undergo two or multi-electron transfer and the mass transport of these redox couples is insignificant in organic solvents. Similar to the I^-/I_3^- redox couple, their redox potential is almost fixed; thus, choosing and using appropriate photosensitizers has become imperative. In addition to this, alternative important and interesting redox mediator ancestors are pure organic compounds such as 2,2,6,6-tetramethyl-1-piperidinyloxy, phenothiazine, tetraphenyldiamine, quinones, and thiolate/disulfide, which have also been exhaustively probed as iodine-free substitutes of redox couples for DSSCs.[27–30] Besides, in addition to inorganic and organic class of redox mediators, metal complexes have been found to be alternative candidates to replace the I^-/I_3^- redox couple because of their reversible electrochemical properties. Moreover, the properties of the metal complex-based redox reactions, *i.e.*, redox potentials can be certainly adjusted by varying the central metal atoms and/or the ligands in order to suit the energy levels of the sensitizers and the conduction band of the semiconductor metal oxide. The transition metal complexes-based redox mediators that are used for DSSC applications include V(V/IV), $[Mn(acac)_3]^{1+/0}$, Fe(III/II), Co(III/II), Ni(IV/III), Cu(II/I), and Os(III/II).[31–37] Despite overcoming many technical problems associated with I^-/I_3^-, the metal complexes typically have sluggish mass transport in solution because of the large molecular size, which is more pronounced in porous semiconductors. Hence, a majority of the metal complex-based DSSCs be able to accomplish improved efficiency under low light conditions (indoor lighting) than that under full light (AM 1.5G, 100 mW cm^{-2}), showing an immense prospective towards the power supplies of device for

portable electronics and wireless sensor network or Internet of Things (IoTs).[38]

Of the various metal complex-based redox couples available, Co(III/II) complex-based redox shuttles have become very fascinating in recent years due to their marked advantages such as non-corrosiveness, non-volatility, ability to achieve a variable electrical potential window while suitably alerting the ligands, and light coloration for less absorption.[15] By using Co(III/II) redox shuttles, the device efficiency has gone up to 13% and 14.3% using porphyrin and metal-free organic dye as sensitizers, respectively.[39,40] Though the Co(III/II) redox couple has many advantages over traditional I^-/I_3^-, the main concern is the recombination losses and mass transport restrictions because of the bulky nature of the Co(III/II) complex. Recombination kinetics of various cobalt complexes suggest that the electron lifetimes are low for $[Co(dtb\text{-}bpy)_3]^{3+/2+}$, slightly lower for $[Co(dm\text{-}bpy)_3]^{3+/2+}$, and the lowest for $[Co(bpy)_3]^{3+/2+}$.[41] On the other hand, their recombination rate constants reduced in the contradictory order, whereby $[Co(bpy)_3]^{3+/2+}$ established the smallest constant for $[Co(dm\text{-}bpy)_3]^{3+/2+}$ and the uppermost constant for $[Co(dtb\text{-}bpy)_3]^{3+/2+}$. This indicates that the structure of the cobalt electrolytes has great significance in attaining the accomplishment of DSSCs. The other main drawback of these electrolytes is that they are cobalt has negative health effects on human beings.[42–44] Cobalt causes breathing problems and severely affects the lungs, including pneumonia, asthma, and wheezing. Studies in animals indicate that exposure to higher amounts of non-radioactive cobalt during pregnancy might influence the health of the embryonic foetus. Birth defects, however, have not been found in children born to mothers who were treated with cobalt for anaemia during pregnancy. Any trace amount of radioactive cobalt, if present, can cause consequential disorders and can damage the tissues, ultimately leading to cancer. Thus, there is a requirement to overcome these drawbacks and the need for new redox shuttles is urgent for DSSCs.

2. Criteria of selection of new redox couples

The redox potential of a redox couple should match to that of the highest occupied molecular orbital (HOMO) of the sensitizer. The minimal driving force required for regeneration is approximated to be about 0.1 eV. This means the more positive redox potential of a redox couple with respect to the HOMO level of the sensitizer so that less energy is lost during the regeneration of the oxidized dye and larger photovoltage would be established (Fig. 1).

- The redox couple must be capable of transporting the charge carriers between the photoanode and the photocathode. The oxidized dye should be quickly reduced to the ground state, once the dye injects electrons to the conduction band of TiO_2. Hence, this aspect should be addressed while designing a new redox couple.
- The redox couples should be designed in such a way so that they have chemical, optical, thermal, electrochemical, and interfacial consistency. They should have long-term stability and should not result in desorption and degradation of the sensitizer.
- The redox couple must assure higher conductivity ($\sim 10^{-3}$ S cm^{-1}) at ambient temperatures and produce excellent contact with the semiconductor layer and the counter electrode.
- For liquid redox couples, care has to be taken such that the solvent has minimal leakage and evaporation of the liquid electrolyte.
- Since the dye has to absorb maximum photons in the visible range, the redox couple should be such that it has no

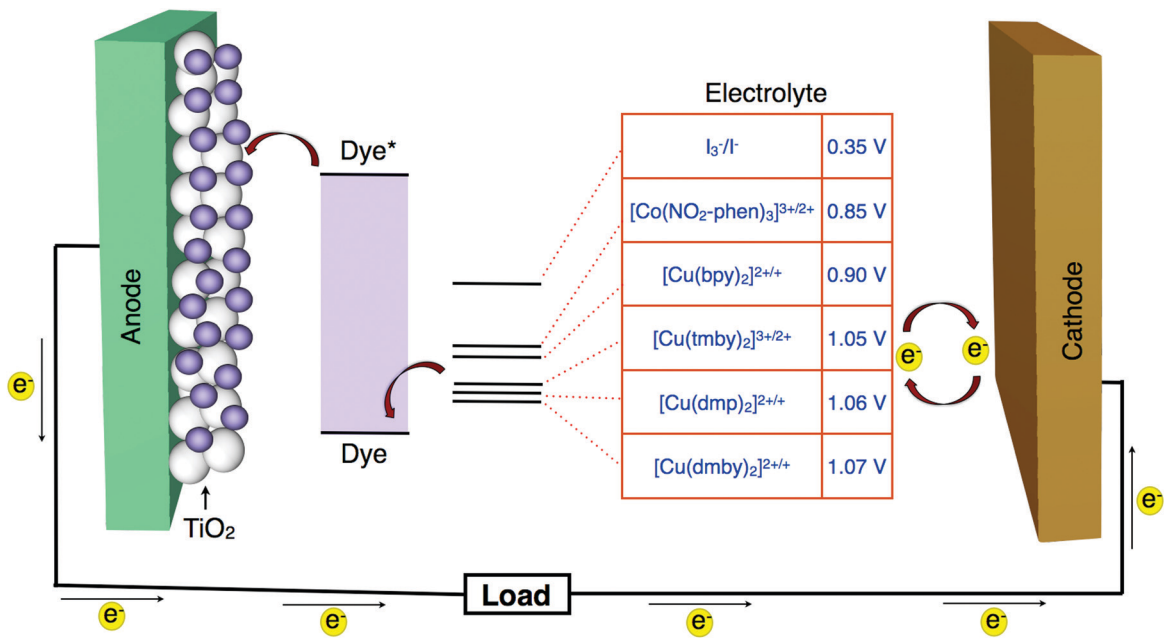

Fig. 1 Schematic energy level diagram of a dye-sensitized solar cell.

absorption or minimal absorption in the visible region, as the absorption of the I^-/I_3^- couple lies in the visible region. If the redox couple has absorption in the visible region, its concentration should be optimized.

By and large, electrolytes are present in all physical states, *i.e.*, liquid, quasi-solid or gel, and solid forms. Efficiencies of up to 14.3% have been accomplished in DSSCs by means of liquid electrolytes (either I^-/I_3^- or $Co^{3+/2+}$ redox couple).[39,40] On the whole, the redox couple is formulated with the combination of parts of a chemical species accessible in various oxidation states. In a photoelectrochemical cell, the redox couple can perform as the reducing or oxidizing agent. The redox couple, additive, and an organic solvent or ionic liquid constitute the liquid electrolyte. Low viscous solvents such as acetonitrile, valeronitrile, and 3-methoxypropionitrile have better interfacial contacts that yield higher efficiency of the device in comparison with gel or solid-state redox electrolytes.[45,46]

3. Cu(II/I) redox couples

Though several redox mediators have been used for DSSC applications with device efficiency crossing 14%, each redox mediator has its own merits and demerits. To overcome the disadvantages of the redox couples, particularly in terms of photovoltaic accomplishments and health issues, Fukuzumi and co-workers have first attempted Cu(II/I) redox couples for DSSC applications.[47] Copper is one of the low-cost metals that are abundantly available in the earth's crust. The application of the Cu(II/I) redox couple to DSSCs was inspired from the electron transfer reactions taking place in the copper complexes, in which copper oscillates between +2 and +1 oxidation states in biological systems.[48–50] Copper complexes present in natural systems are identified as blue copper proteins that serve as electron transfer mediators. In the electron transfer process among photosystems I and II of natural photosynthesis, it involves plastocyanine, a copper system, whereas the electron transfer of the respiratory chain between cytochrome c551 and cytochrome *c* oxidase involves Azulin copper systems. According to the Franck–Condon theory, the transfer of electron is recognized to advance *via* transition state structures, such as the transition of the reactant and product.[51] Hence, for the effective transfer of electron, the metal center should be vibrationally stimulated to match the geometry of the product complex. Electron transfer reactions involve significant reorganizational energies; because of electron density and orbital configuration, there will be internal changes in the bond length and bond angles.[52] However, in copper, such an alteration in the bond lengths in the geometry typically needs a significant energy as copper(I) prefers tetrahedral geometry and copper(II) prefers tetragonal geometry.[53–55] On the other hand, in the case of natural systems, due to the protein system present, the disparity in bond lengths and geometries is minimized, which makes the copper site optimized for quick electron transfer. Cu(II), which possesses d^9 configuration, tends to attain a six-coordinate tetragonal (distorted octahedral) geometry or a five-coordinate

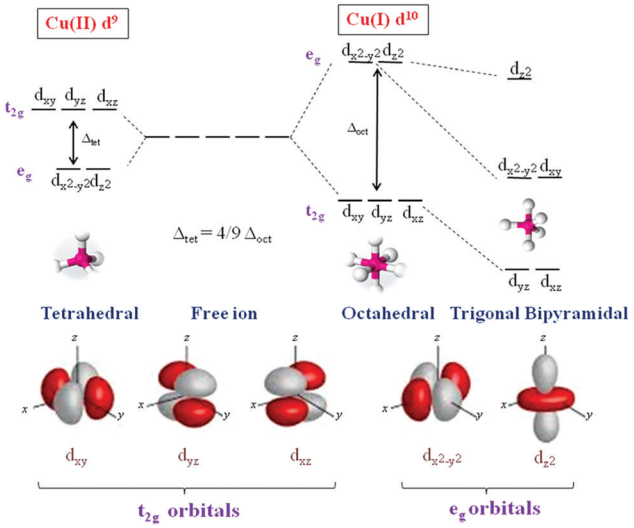

Fig. 2 Orbital splitting pattern of Cu(I) and Cu(II) complexes.

(square pyramidal or trigonal bipyramidal) geometry, and Cu(I), which has a d^{10} configuration, tends to achieve four-coordinate (tetrahedral) geometry (Fig. 2). When electron transfer occurs in the Cu(II/I) system, it is assumed that the rupturing of one or two coordinate bonds and the twisting of the remaining bonds occurs. Thus, the internal reorganizational energies are mainly important in the behavior of copper in electron transfer.[56,57]

Even Jahn–Tellar distortion plays a significant role in Cu(II) complex, which is a dynamic process and suggests that Cu(II) has plastic geometry (Fig. 3). It is evident in plastocyanin, which has a distorted tetrahedral geometry, that an intermediate geometry between Cu(I) and Cu(II) states, which has unusual copper-methionine contact, is found in each oxidation state.[58–61] Plastocyanin belongs to type-1 blue proteins, which has an intense absorption band at 600 nm, whereas this band is

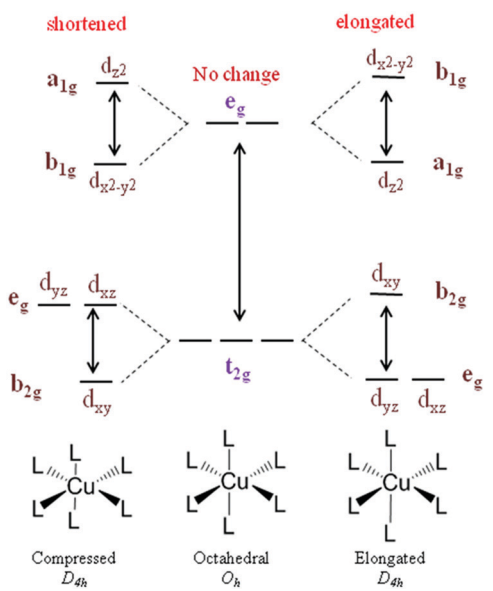

Fig. 3 Jahn–Tellar distortion in Cu(II) complexes.

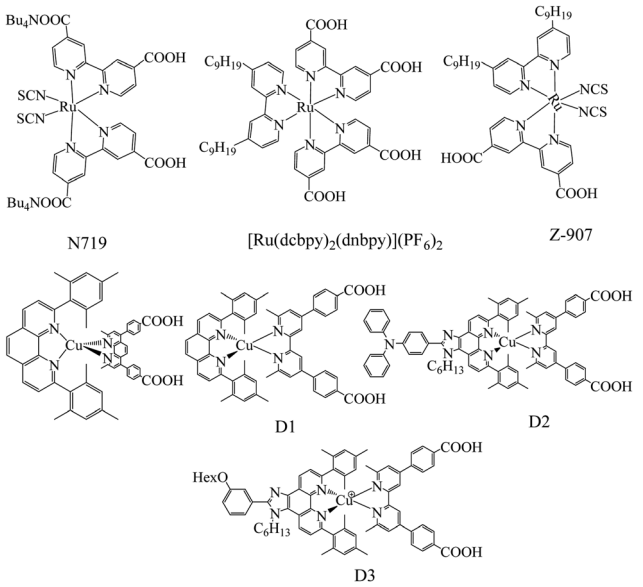

Fig. 4 Molecular structure of metal complex-based sensitizers.

not usually found in other octahedral copper complexes; it has a distinct electron spin resonance spectrum and more importantly, high redox potentials. Keeping this in mind, many copper complexes have been designed and synthesized for DSSC to mimic it for higher redox potentials in achieving high open circuit voltages (V_{OC}) of the cell and high photon conversion efficiency (PCE).[32] Similar to the cobalt complexes, by choosing different ligands on copper, the redox potentials of the complex can be tuned; in turn, V_{OC} will also increase. Many copper complexes with bipyridyl, phenanthroline, and other ligands have been reported and used as redox shuttles using different dyes for DSSCs and significant improvements have been observed in V_{OC} and PCE. Copper complexes not only possess high redox potentials but also require only a minimal driving force ($\sim$0.1 V) for the regeneration of the dye, which reduces the overpotential losses at the electrolyte/dye interface. Even though above 11% efficiency is achieved in DSSCs with metal complexes as redox mediators, this area has not been well explored as much as traditional iodide/triiodide and cobalt complexes. There have been numerous reports based on the studies of iodide- and cobalt-based redox mediators but the studies on copper are lagging behind. The various Cu(II/I) redox shuttles used for DSSC applications are broadly divided into bipyridyl ligands, phenanthroline ligand, and other ligand-based complexes. The various sensitizers that are used for Cu(II/I) redox mediators are presented in Fig. 4–6.

3.1 Bipyridyl ligands

2,2′-Bipyridine ligand has been comprehensively studied in coordination chemistry for the complexation of metal ions since its discovery at the end of the nineteenth century.[62] The ligand has been used in a variety of approaches that include structural coordination chemistry, mainly as dyes and redox shuttles for DSSC applications. In this section, 2,2′-bipyridine ligand Cu(II/I) redox mediators for DSSC applications have been discussed (Fig. 6).

For regenerative photoelectrochemical cells, Bignozzi and co-workers first reported Cu(II/I) redox mediators using a series of bipyridine and pyridyl-quinoline ligands.[63] Due to the decrease in the dark current, it was shown that the copper redox couples achieved higher V_{OC} when compared to the I^-/I_3^- redox couple. It is evidenced from photoelectrochemical studies that maximum incident photon-to-current conversion efficiencies (IPCE) of the order of 35–40% were achieved but it was quite low to consider realistically for substituting the traditional I^-/I_3^- electrolyte. Slower dye reduction, which resulted in lower J_{SC} value, is the prime reason for the lower efficiencies. To suppress the parasitic electron recollection by Cu(II) acceptors, the nature of the dye also plays a prominent role. The exact information regarding the electron transfer processes concerning Cu(II)/(I) species could be identified by further electron transfer processes involving Cu(II)/(I) species containing these electrolytes. In designing novel efficient redox couples, understanding the relationship between the redox properties, mediator structure, and electron transfer kinetics is an important task.

Lars Kloo and co-workers have designed and synthesized a novel copper redox couple $[Cu(bpye)_2]^{2+/+}$ (bpye = 1,1-bis(2-pyridyl)ethane) and employed it in DSSC in combination with a metal-free organic dye (LEG 4).[64] The photovoltaic measurements in which both IPCE and *I–V* were measured at various light intensities and compared with the cobalt redox couple, $[Co(bpy)_3]^{3+/2+}$ (bpy = 2,2′-bipyridine). The copper complex is highly stable under electrochemical stress. Higher power conversion efficiencies were obtained when evaluated for cobalt redox couple under similar test cell conditions in all three light intensities of 1.0, 0.5, and 0.1 sun. At 1 sun, using the copper redox couple gave a PCE of 9.0%, whereas cobalt gave 7.7%. Similarly, all other photovoltaic parameters recorded for the copper complex were higher compared to that of the cobalt complex. The higher value of V_{OC} may be attributed to a couple of reasons such as the change in the electrolyte redox potential and the recombination loss reactions at the interface. The difference in the redox potential of $[Cu(bpye)_2]^{2+/+}$ over $[Co(bpy)_3]^{3+/2+}$ by 30 mV also contributes to better V_{OC}. The higher J_{SC} may be attributed to better electrolyte charge transport and quicker dye regeneration by the Cu complex. Long-term stability studies suggest that the device loses efficiency from 9 to 6% within 20–40 h, after which the device is photochemically stable up to 700 h. These results suggest that the copper complex-based devices have potential for indoor applications.

In an another study, Freitag and co-workers, to maintain the driving force to be sufficiently less for dye regeneration and quicker electron back transfer to the oxidized dye with the redox couple, synthesized a couple of Cu **bipyridyl** complexes, *i.e.*, $[Cu(dmby)_2]TFSI_{2/1}$ (dmby = 6,6′-dimethyl-2,2′-bipyridine) and $[Cu(tmby)_2]TFSI_{2/1}$ (tmby = 4,4′,6,6′-tetramethyl-2,2′-bipyridine) as promising redox couples in DSSC.[65] They compared their performance with that of the previously reported copper complex of $[Cu(dmp)_2]TFSI_{2/1}$ (dmp = bis(2,9-dimethyl-1,10-phenanthroline)). Using Y123 as a sensitizer and

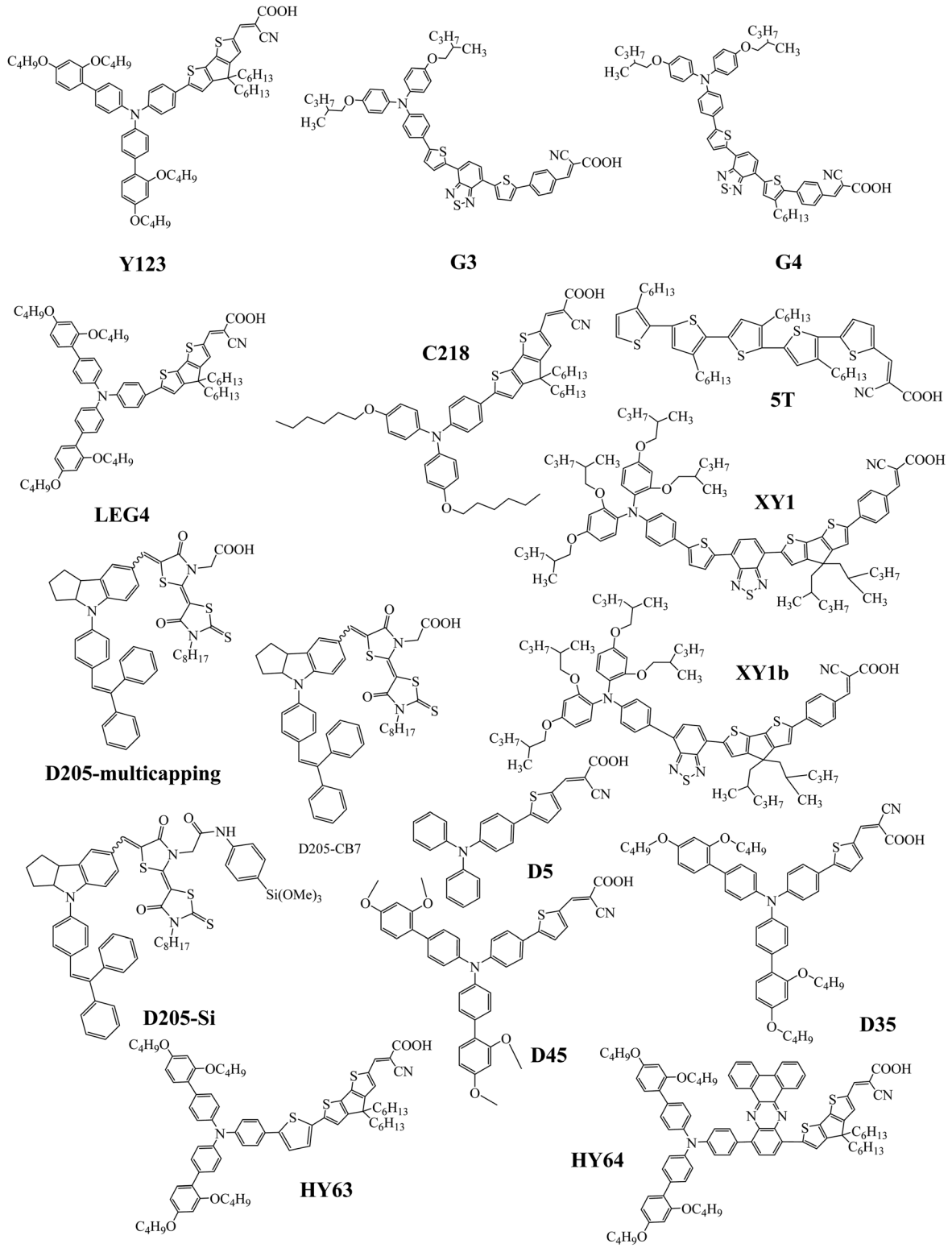

Fig. 5 Molecular structure of metal-free organic sensitizers.

$[Cu(tmby)_2]^{2+/+}$, $[Cu(dmby)_2]^{2+/+}$, and $[Cu(dmp)_2]^{2+/+}$ as electrolytes, relatively higher solar to power conversion efficiencies were obtained, *i.e.*, 10.3%, 10%, and 10.3%, respectively, under 1000 W m^{-2} AM1.5G illumination. The present copper redox mediators have showed higher efficiencies due to the sufficient regeneration of the oxidized dye almost to the unit yield by a driving force as low as 0.1 V, which is because of lesser reorganization energy between Cu(I) and Cu(II) species. Higher

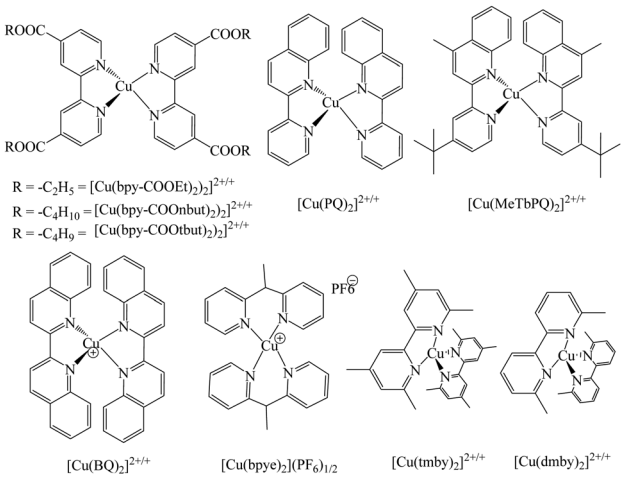

Fig. 6 Molecular structure of bipyridyl copper complexes.

photovoltages of above 1.0 V were attained in the series of copper complexes without compromising the photocurrent densities. Though the driving forces were small, fast regeneration of the dye, *i.e.*, 2–3 μs, was obtained for both the complexes. With the evidence of longer lifetimes observed for $[Cu(tmby)_2]TFSI_{2/1}$, the electron back transfer rates were much slower, which would be an added advantage. It was predicted for Cu complexes that very low inner-sphere reorganization energies were obtained when compared to that of the Co complexes. For Co(II) complexes, the inner-sphere reorganization energy (λ_{in}) values lies between 0.52–0.63 eV (when Co(II) is considered as low spin) and Co(II) lies in 1.39–1.78 eV when considered in the high spin sate. Since the inner sphere reorganization energy has proven to limit dye regeneration process in Co complexes as redox mediators, this group reported the same in Cu complexes. The low reorganization energy arises because these copper complexes originate from very small changes in the ligand-copper distance upon oxidation, which are only ~2% for the Cu ligand (against ~10% for the Co-ligand complexes). The spherically symmetric Cu(I) $3d^{10}$ configuration is much less sensitive than Co(II) for structural deformations in the ligand coordination sphere. Since the reorganizational energies of these complexes are less, the driving force for dye regeneration could be kept small to attain superior photo voltages. Also, these copper complexes based DSSC are anticipated to be favorable for indoor applications since the photovoltages are as high as 1 V with 0.2 Sun illumination. Also, they suggested that a further improvement in the device efficiency could be possible by improving the fill factor by better counter electrode materials.

In a seminal work, Li *et al.* also applied the $[Cu(dmby)_2]BF_{4\ 2/1}$ redox couple in combination with Y123 as a sensitizer.[66] The single crystal XRD studies suggest that the Cu(I) complex has a distorted tetrahedral geometry with a dihedral angle of 80.9° and Cu(II) complex crystal has a distorted tetrahedral geometry with a dihedral angle of 62.6° (Fig. 7). The device has demonstrated a considerable increase in the V_{OC} of 1048 mV and a short circuit photocurrent density of J_{SC} 14.4 mA cm^{-2} with a high power

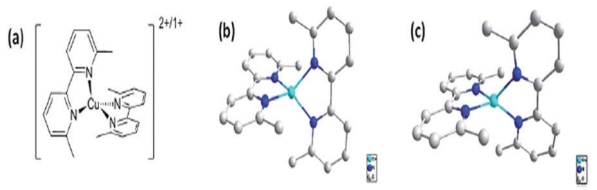

Fig. 7 (a) Chemical structure of $[Cu(dmbp)_2]^{2+/2}$. (b) Single crystal structure of $Cu(dmbp)_2^{+}$ and (c) $Cu(dmbp)_2^{2+}$ (ref. 66).

conversion efficiency of 10.3% under AM1.5G condition. They also compared the device with the I^-/I_3^- and Co(III/II) redox mediators under similar test cell conditions. The study suggested that as the driving force reduced from I^-/I_3^- to Cu(II/I) redox mediators, the V_{OC} was enhanced from 724 to 1048 mV while the J_{SC} was reduced from 15.8 to 14.4 mA cm^{-2}. A small driving force of 0.11 eV is sufficient to regenerate the oxidized dye with minimal energy loss (Fig. 8). Very rapid electron self-exchange between Cu(I) and Cu(II) complexes is noticed because of stacking interactions between the neighboring aromatic ligands, which tends to a small alteration in the structure of the complex. They also noticed that the reduction process was relatively slower when compared to oxidation. The redox potential of the copper complex was found to be 0.97 V *vs.* NHE, which is far more positive than that of the I^-/I_3^- and cobalt(III/II) redox couples. The corresponding increment in V_{OC} can be explained by the synergy of recombination and shifts in the conduction band. They observed a comparatively low reduction rate for the $[Cu(dmbp)_2]^{2+/+}$ system and incompetent catalytic activity between platinum and the copper complex shuttle at the counter electrode, which is responsible for the low FF.

The addition of additives such as 4-*tert*-butyl pyridine (TBP) in redox couples decreases the dark current and enhances the device efficiency.[67,68] Wang *et al.* have studied the role of TBP additive in the $[Cu(dmbp)_2]^{2+/1+}$ redox shuttle and reported higher efficiencies in combination with the Y123 sensitizer both in the liquid and solid states.[69] The addition of 0.6 M concentration of TBP to the $[Cu(dmbpy)_2]^{2+/+}$ couple causes a hasty ligand substitution reaction, which results in the $[Cu(TBP)_4]^{2+}/[Cu(dmbpy)_2]^{+}$ redox species in solution. This has

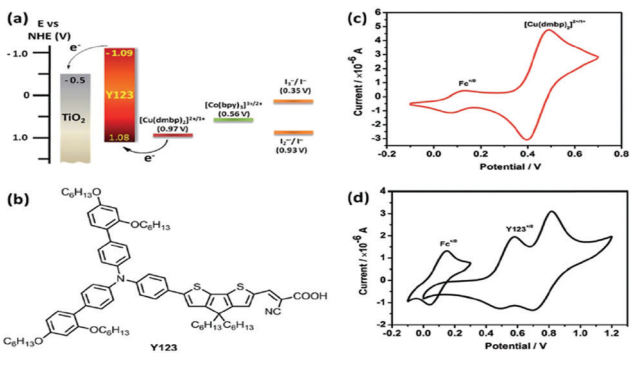

Fig. 8 (a) Schematic energy levels of Y123-sensitized TiO_2 film with different redox systems. (b) Chemical structure of the Y123 sensitizer. (c) Cyclic voltammogrammes of the $Cu(dmbp)^{2+}$ complex and Y123 adsorbed on the TiO_2 film (ref. 66).

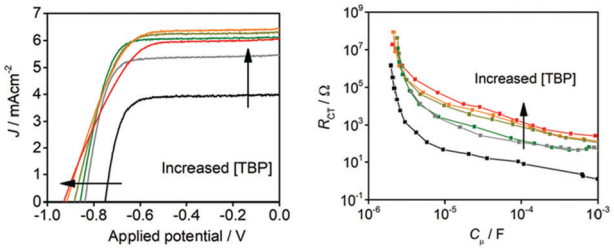

Fig. 9 (a) J–V characteristics of the DSSC devices using various concentrations of TBP. (b) Plots of the charge transfer resistance (RCT) *vs.* the chemical capacitance (Cm) of the devices to demonstrate the effect of TBP on the recombination kinetics [0 M (black), 0.1 M (gray), 0.2 M (green), 0.3 M (dark yellow), 0.4 M (orange), and 0.5 M (red)] (ref. 69).

been confirmed by the absorption, electrochemical, and ^{1}H NMR studies. Previous reports of the $[Cu(dmbpy)_2]^+$ species show the quantitative regeneration of dyes with minimal driving force, which is important for getting better efficiencies. The presence of $[Cu(TBP)_4]^{2+}$ and free TBP in the redox electrolyte both influence the J_{SC} and V_{OC}. The losses in V_{OC} are due to the negative shift of the solution potential due to ligand exchange reaction at 270 mV. The enhanced short-circuit current due to the addition of TBP is due to the reduced recombination (Fig. 9). By the suitable tuning of ligand substitution, the photovoltage is improved without a marked loss in the photocurrent.

In another study, Freitag and co-workers have examined the recombination of the injected electrons with the oxidized redox species and the regeneration behavior of copper electrolytes using D5, D35, and D45 metal-free organic sensitizers, which have various degrees of blocking factor.[70] The Cu(II/I) redox couples used in this study are $[Cu(dmby)_2]^{2+/+}$, $[Cu(tmby)_2]^{2+/+}$, $[Cu(eto)_2]^{2+/+}$ (eto = 4-ethoxy-6,6′-dimethyl-2,2′-bipyridine), and $[Cu\text{-}(dmp)_2]^{2+/+}$ (dmp = bis(2,9-dimethyl-1,10-phenantroline)). The driving forces were as low as 0.1 eV, which allows the efficient regeneration of the oxidized dye, in which the low reorganization energy of (λ = 0.31–0.34 eV) supports to this fact and the electron transfer regeneration reaction lies in the Marcus normal regime (Fig. 10).

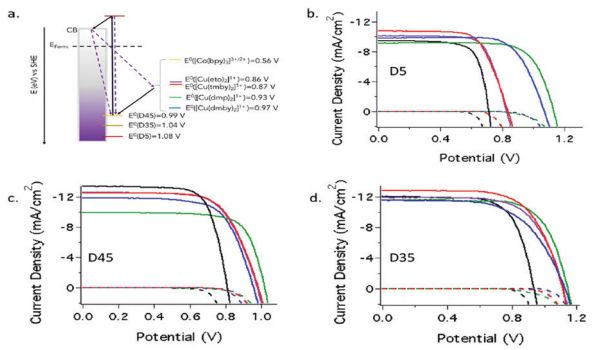

Fig. 10 (a) Schematic energy diagram represents the highest occupied molecular orbitals (HOMO) of D5, D35, and D45 dyes with the formal redox potentials of the Cu(I) species and (b–d) current density vs applied potential curves under dark and 100 W cm^{-2} AM1.5G illumination for DSSC devices measured with a mask aperture of 0.158 cm^2. ($[Cu(dmby)_2]^{2+/+}$, blue; $[Cu(tmby)_2]^{2+/+}$, red; $[Cu(eto)_2]^{2+/+}$, purple; $[Cu(dmp)_2]^{2+/+}$, green; $[Co(bpy)_3]^{3+/2+}$, black) (ref. 70).

On the other hand, the presence of TBP for Cu(II) species in the electrolyte medium will have altered charge recombination kinetics due to the penta-coordinated complex (λ = 1.23–1.40 eV). From the large driving force for the electrons, charge recombination in the Marcus inverted regime could have been expected; instead, it has Marcus normal regime due to higher reorganization energies. When compared to the reference cobalt electrolyte, the copper electrolyte had a better recombination resistance and electron lifetime values. When D35 was coupled with $[Cu\text{-}(dmp)_2]^{2+/+}$ without compromising on the short circuit current density, a record open circuit voltage of 1.14 V was reached. The D5 sensitizer, which does not exhibit recombination, prevents steric units when coupled with $[Cu\text{-}(dmp)_2]^{2+/+}$ and $[Cu(dmby)_2]^{2+/+}$ and could reach an efficiency of 7.5% with 1.5G full sun illumination and 1.13 V as the open circuit voltage. On the other hand, an intermediate degree of blocking factor, *i.e.*, D45, observed only 1.02 V under similar test cell conditions.

Ladislav Kavan and co-workers have studied the performance of three copper complexes, *i.e.*, $[Cu(dmp)_2]^{2+/+}$, $[Cu(dmby)_2]^{2+/+}$, and $[Cu(tmby)_2]^{2+/+}$ as redox mediators on diverse electrodes and different electrolyte solutions using impedance spectroscopy and cyclic voltammetry using dummy cells.[71] When compared to the activity of platinum, the graphene-based catalyst showed higher activity compared to PEDOT and outperformed that of platinum. In the presence of TBP, the diffusion rate and charge transfer kinetics slow down significantly; this effect was not observed in cobalt electrolytes and can only be seen in copper-based mediators because of the coordination sphere of Cu(II) species due to structural and substitutional changes. From PEDOT/PEDOT symmetrical devices, they prepared Zombie cells, which showed improved charge transfer rate and improved diffusion resistance. As a result of the electrochemical oxidation of the parent Cu(I) complex, they prepared electrochemically clean Cu(II) bipyridine for the first time. These results suggest that the electrochemically-grown clean Cu(II)-bipyridine complex is demonstrated for practical dye-sensitized solar cells.

In another study, Ladislav Kavan and co-workers developed an innovative synthetic procedure to make electrochemically and optically clean $[Cu(tmby)_2]TFSI$ and $[Cu(tmby)_2]TFSI_2$ in a mixture (tmby = 4,4,6,6-tetramethyl-2,2-bipyridine; TFSI = trifluoromethylsufonylimide).[72] Faster diffusion transport rate in solution and better charge transfer rate was observed with this copper electrolyte at the counter electrode (PEDOT). They examined this with 4 pyridine bases as electrolyte additives, *i.e.*, 4-*tert*-butylpyridine, 2,6-bis-*tert*-butylpyridine, 4-methoxypyridine, and 4-(5-nonyl)pyridine. It was found that in $[Cu(tmby)_2]^{2+/+}$, base-specific electrochemical properties were observed, whereas in the cobalt complexes as electrolyte, this was not found. 2,6-Bis-*tert*-butylpyridine has the smallest effect on the mediators' electrochemistry because of steric hindrance and ineffective V_{OC} enhancement. The basicity of the used pyridine derivatives has a direct influence on the charge transfer rates and diffusion resistance. Solar cells are fabricated with the Y-123 dye and the power conversion efficiency is evaluated in the presence of different bases. Coordination ability dependence on basicity

can be tuned by optimizing the pyridine bases' Cu-mediated solar cells. This further allows the tuning of the charge transfer rate at the counter electrode and mass transport in the electrolyte solution. 4-(5-Nonyl)pyridine outperformed other bases in the photoelectrochemical properties, where 9.4% efficiency could be achieved.

Enhanced device efficiency were obtained using Cu(II/I) redox shuttles due to the higher V_{OC} values but a major bottleneck for the further improvement of PCE is that the J_{SC} values are moderate. In order to improve the J_{SC} values, the sensitizer should have absorption till the red or NIR region. Grätzel and co-workers modified the dye Y123 by introducing either benzothiadiazole (BTZ) HY63 or phenanthrene-fused-quinoxaline (PFQ) HY64 as the auxiliary acceptor to push the absorption to the near-IR region.[73] The spectral response of both HY63 and HY64 sensitizers was improved in the red region of the spectrum in comparison with that of the Y123 sensitizer. The photoelectrochemical properties of both the dyes along with the standard Y123 dye were compared using $[Cu(tmby)_2]^{2+/+}$ $(TFSI)_{1/2}$ redox couple under similar test cell conditions (Fig. 11). The device studies suggest that the HY64 sensitizer outperforms its counterparts with a PCE of 12.5%, which is the highest efficiency reported for the Cu(II/I) redox couple under one sun irradiation. The energy levels and absorption onsets are identical but the high efficiency of PFQ over BTZ due to decreasing charge recombination ensuing in the near quantitative collection of photogenerated charge carriers. In addition to this, the HY64 sensitizer showed greater stability under continuous light soaking at 60 °C. Furthermore, see-through devices attain a PCE of 11.2%, demonstrating semi-transparent photovoltaics.

The co-sensitization of different sensitizers having absorption in the harmonizing spectral region is another way to enhance the device efficiency. Freitag *et al.* combined two thoughtfully designed sensitizers D35 and XY1 with the $[Cu(tmby)_2]^{2+/+}$ redox couple.[74] The devices prepared by the combination of D35 and XY1 dyes in 4 : 1 ratio gave the best performance as the external quantum efficiency surpassed 90% across the whole visible area from 400 to 650 nm with the PCE reaching 11.3%, which is a new record for a system based on a copper electrolyte using the co-sensitization concept. Once again in the present co-sensitization system, the driving force necessary to regenerate the oxidized dyes is only 0.1–0.2 eV. With the help of artificial fluorescent lighting using Osram 930 warm-white fluorescent light tube, a power generation of 15.6 and 88.5 μW cm^{-2} is accomplished at 200 and 1000 lux, respectively, which translates to a PCE of 28.9%.

Recently, Robertson and co-workers have mixed a less expensive 5T dye with the better performing XY1 dye to engineer the co-sensitized devices using $[Cu(tmby)_2]^{2+/+}$ redox mediator (Fig. 12).[75] At 1 sun condition, the co-sensitized device showed a comparable power conversion efficiency of XY1 (avg. 9.1%) but exhibited higher conversion at 0.1 sun (avg. 9.4 *vs.* 8.6%). Under low light conditions with the help of artificial fluorescent lighting, the co-sensitized device was further assessed and showed a PCE as high as 29.2% at 1000 lux, amid the highest reported device efficiency. Improved performance at 0.1 sun can be perhaps attributed to the drift in the equilibrium between charge recombination and mass transport in the electrolyte and the interface. Cao *et al.* reported a different device architecture, in which PEDOT acts as the counter electrode dye-impregnated mesoporous TiO_2 electrode and is directly contacted without using any spacer.[76] The novel architecture diminishes the diffusion channel of the redox mediator to purely the TiO_2 film satisfying the Warburg resistance. Co-sensitization of metal-free organic dyes Y123 and XY1b with the liquid $[Cu(tmby)_2]^{2+/+}$ redox mediator reached an efficiency of 13.1% using the advanced device architecture under standard conditions (J_{SC} 15.74 mA cm^{-2}, V_{OC} 1.050 mV, and FF of 0.79). The efficiency was further enhanced to 32% under artificial indoor lighting at 1000 lux with an output power density of 101.2 mW cm^{-2}, which is the highest reported DSSC device efficiency to date (Fig. 13). Overall, the co-sensitization concept using Cu(II/I) redox mediators that function well under indoor

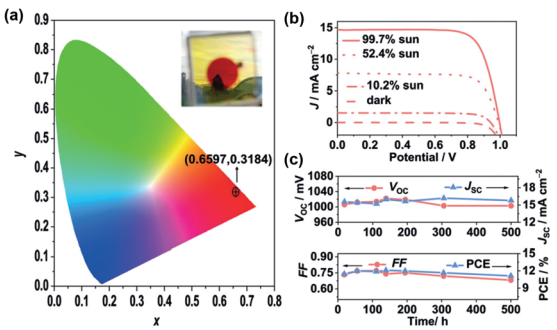

Fig. 11 (a) Stability evaluation of semi-transparent devices. (a) Color coordinate of 4 μm-thick HY64-sensitized TiO_2 film in permutation with copper electrolyte-$[Cu(tmby)_2]^{2+/2}$ in the CIE 1931 *XY* chromaticity diagram. The inner photograph represents the film state device. (b) Current density (*J*)–voltage (*V*) curves of DSSCs with the HY64 dye adsorbed on the scattering layer of the free TiO_2 film, employing $[Cu(tmby)2]^{2+/1+}$ as the redox shuttle under various light intensities. (c) Evaluation of V_{OC}, J_{SC}, FF, and PCE of the HY64 dye-based DSSCs under AM1.5 sunlight (100 mW cm^{-2}) during continuous light soaking at 60 °C for 500 h (ref. 73).

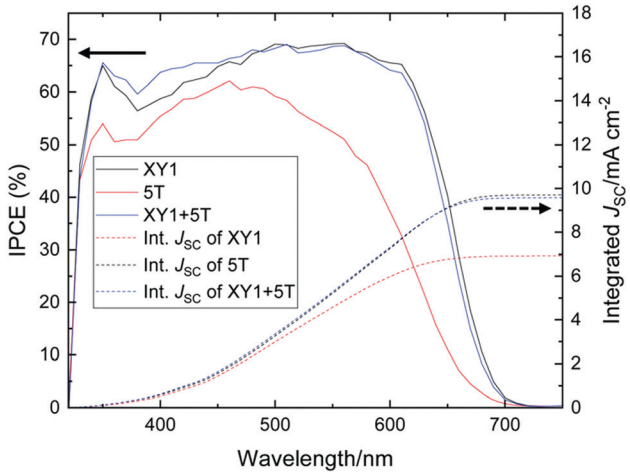

Fig. 12 IPCE curves of XY1 (black), 5T (red), and XY1 + 5T (blue)-sensitized DSSCs. The dotted lines are the integrated current density values (ref. 75).

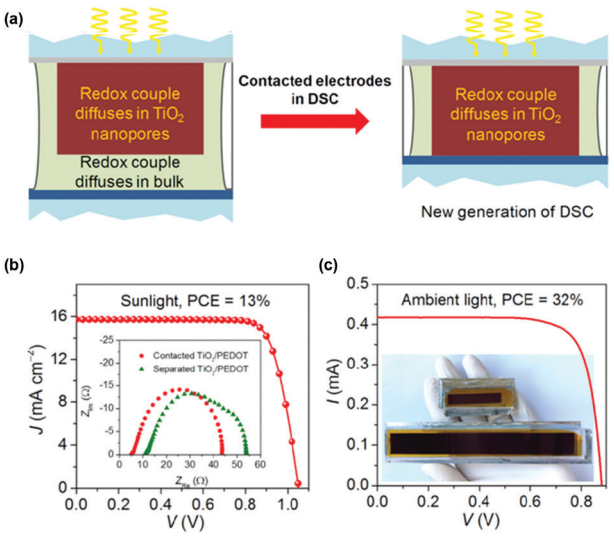

Fig. 13 (a) Pictorial representation for the new generation of DSSCs to prevent electrical shunts. The redox couple has to diffuse in both the mesoporous film and the bulk phase of the electrolyte. (b) *J*–*V* characteristics curves. Inset figure represents the impedance analysis of the contacted and separated TiO_2/PEDOT. (c) *J*–*V* spectra for the co-sensitization of mesoscopic TiO_2 by XY1b/Y123 and a Cu(II)/Cu(I)-based electrolyte and the emitted power density spectrum using white fluorescent tube light. Inset picture of the two DSSCs with different photoactive areas of 2.80 and 20.25 cm^2, respectively (ref. 76).

lighting are of potential practical curiosity as they can operate as electric power supplies for devices with portable electronics and wireless sensor networks or Internet of Things.

The fancy efficiencies of DSSC devices were obtained using a liquid redox electrolyte but the durability of the device was not sufficient mainly due to the utilization of volatile acetonitrile solvent. Either polymer gel or solid-state hole conductors may provide a probable solution in this direction. The low efficiency of DSSC devices using solid-state hole conductors is due to inadequate nanopore filling, crystallization of hole-transport materials penetrated in the nanocrystalline TiO_2, and low conductivity at ambient temperatures. Boschool and co-workers used a hole transport material composed of a blend of $[Cu(tmby)_2](TFSI)_{2/1}$ using metal-free organic dye Y123 and reported a record efficiency of 11%.[74,78] In contrast, using 0.06 M $[Cu(tmby)_2](TFSI)_2$, 0.2 M $[Cu(tmby)_2](TFSI)$, 0.1 M LiTFSI, and 0.6 M 4-*tert*-butylpyridine (TBP) in acetonitrile with PEDOT on FTO as the counter electrode obtained only 9.3 ± 0.3% efficiency under standard AM1.5G conditions (Fig. 14).

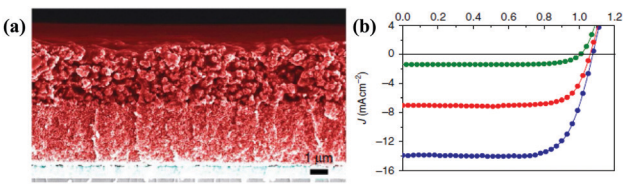

Fig. 14 (a) Cross-sectional SEM image without the counter electrode. (b) *J*–*V* curves of a champion DSSC under standard illumination of AM1.5G at 1000 (royal blue), 500 (red), and 100 W m^{-2} (olive) (ref. 78).

The high efficiency of the solid-state device over the liquid-based redox mediator is due to the slow evaporation of the acetonitrile solvent of electrolyte in ambient air, which encourages the solidification of $[Cu(tmby)_2]^{2+/+}$ and provides better interfacial contact, which is not possible during rapid evaporation. The time-resolved laser photolysis studies indicate that electron injection from the excited state of the dye into the TiO_2 conduction band is 25 ps against dye regeneration by taking the electron from the redox mediator, which was 3.2 ms (Table 1).

In the presence of a range of titania/dye/electrolyte modifications, Marcin Ziolek's group studied the photovoltaic accomplishment of solar cells sensitized with an indoline-based D205 dye and its new derivative containing alkoxysilyl anchoring the constituent (D205Si) using $[Cu(tmby)_2](TFSI)_{1/2}$ electrolyte-mediated systems.[79] To encapsulate the dye molecules, cucurbit[7]uril (CB7) was used, an electronically insulated layer was created, and electron interception was suppressed by the electrolyte, which led to an increase in the lifetime of the

Table 1 Photovoltaic data of copper(I/II) redox shuttles using bipyridine ligands

Electrolyte	Dye	J_{SC}[a]	V_{OC}[a]	FF[a]	η (%)	Ref.
$[Cu(bpye)_2]^{2+/+}$	LEG4	13.8	0.90	0.71	9.0	64
		7.3	0.89	0.76	9.9[b]	
$[Cu(tmby)_2]^{2+/+}$	Y123	15.5	1.04	0.64	10.3	65
$[Cu(dmby)_2]^{2+/+}$	Y123	14.1	1.07	0.68	10.0	65
$[Cu(dmby)_2]^{2+/+}$	Y123	14.4	1.05	0.68	10.3	66
$[Cu(eto)_2]^{2+/+}$	D5	10.12	0.83	0.72	6.0	70
$[Cu(eto)_2]^{2+/+}$	D45	12.59	0.98	0.67	8.21	70
$[Cu(eto)_2]^{2+/+}$	D35	11.93	1.12	0.66	8.84	70
$[Cu(tmby)_2]^{2+/+}$	D5	10.79	0.98	0.67	6.61	70
$[Cu(tmby)_2]^{2+/+}$	D45	12.52	0.98	0.67	8.3	70
$[Cu(tmby)_2]^{+/2+}$	D35	12.81	1.11	0.66	9.44	70
$[Cu(dmby)_2]^{2+/+}$	D5	9.85	1.07	0.71	7.53	70
$[Cu(dmby)_2]^{2+/+}$	D45	11.85	0.96	0.68	7.71	70
$[Cu(dmby)_2]^{2+/+}$	D35	11.53	1.13	0.60	7.84	70
$[Cu(tmby)_2]^{2+/+}$	Y123	13.33	1.03	0.75	10.03	73
$[Cu(tmby)_2]^{2+/+}$	HY63	13.71	0.99	0.76	10.3	73
$[Cu(tmby)_2]^{2+/+}$	HY64	15.76	1.03	0.77	12.5	73
$[Cu(tmby)_2]^{2+/+}$	D35 + XY1 (4 : 1 ratio)	16.20	1.10	0.68	11.3	74
		0.14	0.80	0.80	28.9[b]	74
$[Cu(tmby)_2]^{2+/+}$	XY1	11.4	1.05	0.76	9.1	75
$[Cu(tmby)_2]^{2+/+}$	5T	9.90	0.97	0.77	7.5	75
$[Cu(tmby)_2]^{2+/+}$	XY1 + 5T	11.80	1.04	0.74	9.1	75
$[Cu(tmby)_2]^{2+/+}$	XY1 + 5T	0.13	0.86	0.78	29.2[b]	75
$[Cu(tmby)_2]^{2+/+}$	Y123 + XY1b	15.74	1.05	0.79	13.1	76
		0.004	0.88	0.77	31.8[b]	76
$[Cu(tmby)_2]^{2+/+}$	Y123	13.87	1.08		11.0	77
$[Cu(tmby)_2]^{2+/+}$	D205 multicapping	6.33	0.89	0.81	4.51	79
$[Cu(tmby)_2]^{2+/+}$	D205-CB7	5.86	0.92	0.82	4.38	79
$[Cu(tmby)_2]^{2+/+}$	D205-Si	5.76	0.89	0.77	3.92	79
$[Cu(tmby)_2]^{2+/+}$	D205-Si multicapping	6.22	0.88	0.80	4.37	79
$[Cu(tmby)_2]^{2+/+}$	D205-Si CB7	5.98	0.95	0.78	4.41	79
$[Cu(tmby)_2]^{2+/+}$	Y123	10.50	1.07	0.71	8.01	79
$[Cu(tmby)_2]^{2+/+}$	Y123 multicapping	10.82	1.03	0.71	7.86	79
$[Cu(tmby)_2]^{2+/+}$	Y123-CB7	9.96	1.01	0.72	7.21	79
$[Cu(tmby)_2]^{2+/+}$	D205	6.52	0.89	0.79	4.43	79
$[Cu(tmby)2]^{2+/+}$	LG4	8.33	0.91	0.67	5.07	80
$[Cu(tmby)2]^{2+/+}$	LG5	6.86	0.89	0.71	4.36	80
$[Cu(dmp)_2]^{2+/+}$	LG4	6.89	0.89	0.65	3.98	80
$[Cu(dmp)_2]^{2+/+}$	LG5	5.06	0.86	0.69	3.30	80

[a] Error limits: J_{SC} = ±0.20 mA cm^{-2}, V_{OC} = ±0.30 mV, FF = ±0.03, and η = ±0.1. [b] Device efficiency measurement at 1000 lux.

electron in the titania conduction band. As illustrated, the lifetime of the electron was increased to 6.5 ms from 2.2 ms by encapsulating with CB7 at 0.9 V bias voltage of the D205 cells. To prevent electron recombination and reduce dye desorption, molecular multicapping was optimized. Hence, in a majority of cases, preferably when applied to alkoxysilyl anchoring derivative, by modifying the interface, it was noticed that the photovoltaic performance was enhanced. For the given system and with allusion $[Co(bpy)_3](TFSI)_{3/2}$, the charge transfer process of the redox couple was investigated by electrochemical impedance spectroscopy, nanosecond and femtosecond transient absorption studies, and small light perturbation electron lifetime measurements. It was noticed that indoline dyes were regenerated rapidly by the Cu-based redox couple. Because of lesser J_{SC} and reduction in the V_{OC} values, the photovoltaic performance of the Cu-based electrolyte with indoline dyes is much lesser than that of the Y123 dye, which is evident from the data. In DSSC, the porphyrins are another interesting class of sensitizers, in which the device efficiency has reached up to 13% using the Co(III/II) redox couple (V_{OC} 0.91 V and J_{SC} 18.1 mA cm^{-2}). Still, there is a chance to enhance the V_{OC} by reducing the driving force for charge recombination of the porphyrin-based sensitizers. This can be achieved by applying the Cu(II/I) redox mediators. Recently, Imahori and co-workers applied two donor–π–acceptor porphyrin sensitizers, *i.e.*, LG4 and LG5 in combination with the $[Cu(tmby)_2]^{2+/+}$ redox mediators.[80] LG4 dye has showed better device performance of 5.07% over the LG5 sensitizer (4.36%), which is the highest efficiency of a porphyrin-based sensitizer with copper redox mediators to date.

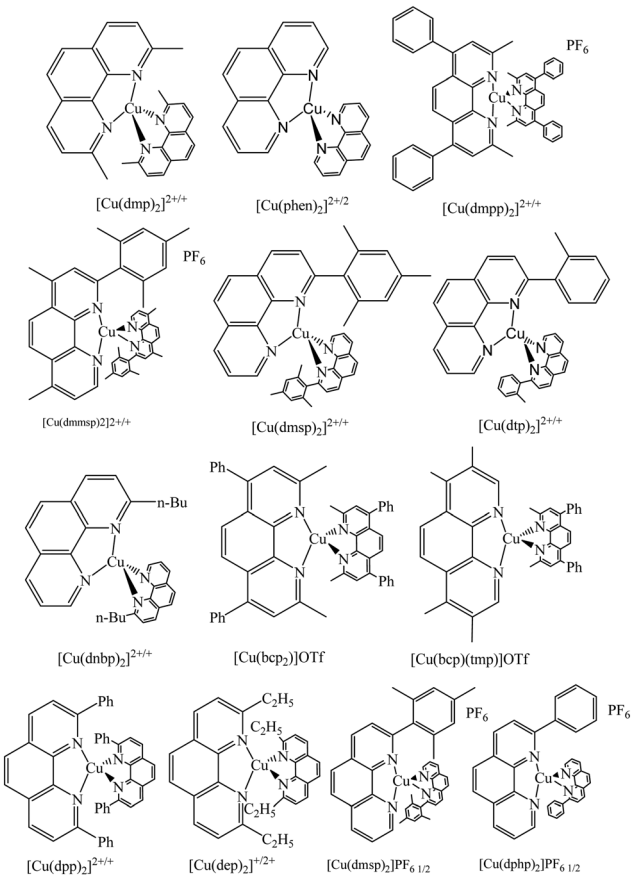

Fig. 15 Molecular structure of the 1,10-phenanthroline ligand-based copper complexes.

3.2 Phenanthroline ligands

Similar to 2,2′-bipyridine ligands, another interesting ligand in coordination chemistry is 1,10-phenanthroline (Phen), which is used in different fields of chemistry.[81] Indeed, a great variety of Cu(II) derivatives using substituted phenanthroline ligands have been applied in DNA binding and photocleavage studies.[82,83] However, Cu(I) complexes of phenanthroline ligand derivatives have not been much explored in the literature.[84,85] The copper complexes of both I and II oxidation states using phenanthroline ligand derivatives as redox couples were also studied for DSSC applications (Fig. 15).

Shunichi Fukuzumi and group reported the copper complex $[Cu(dmp)_2]^{2+/+}$ [dmp = bis(2,9-dimethy-1,10-phenanthroline)] as the redox shuttle in the DSSC for the first time to replace the I^-/I_3^- redox couple.[47] This has great advantage since dmp ligands are commercially available and the copper complex of dmp can be easily made in one step. Structural modification between the copper(I) and copper(II) complexes is minimized, giving a capable approach for developing the DSSC. Along with $[Cu(dmp)_2]^{+/2+}$, two other copper complexes were reported, *i.e.*, $[Cu(SP)(mmt)]^{0/-}$[(SP)(mmt) = (−)-sparteine-*N*,*N*′](maleonitriledithiolato-*S*,*S*′) and ($[Cu(phen)_2]^{2+/+}$ [phen = bis(1,10-phenanthroline)]). Under solar-simulated illumination (100 mW cm^{-2}), the power conversion efficiency of the DSSC was found to be 0.1%, 1.4%, and 1.3% for $[Cu(phen)_2]^{2+/+}$, $[Cu(dmp)_2]^{2+/+}$, and $[Cu(SP)(mmt)]^{0/-}$ complexes, respectively. For the $[Cu(dmp)_2]^{2+/+}$ redox couple, a maximum efficiency of 2.2% was realized under low light intensity of 20 mW cm^{-2}, and higher V_{OC} were observed when compared to that of the I^-/I_3^- redox couple. Low photovoltaic properties for the $[Cu(phen)_2]^{+/2+}$ redox couple may be attributed to the slowest self-exchange rate and the lowest redox potential of −0.10 V. In the case of the $[Cu(SP)(mmt)]^{0/-}$ redox couple, both J_{SC} and V_{OC} are improved probably because of the faster self-exchange rate of the electron and higher redox potential of 0.29 V. But, in the case of $[Cu(dmp)_2]^{2+/+}$, the J_{SC} value is smaller than that of $[Cu(SP)(mmt)]^{0/-}$ even though the electron self-exchange rate is much faster than that of $[Cu(SP)(mmt)]^{0/-}$ perhaps due to the considerably lesser driving force of electron transfer from $[Cu(dmp)_2]^{2+/+}$ to the dye cation compared to $[Cu(SP)(mmt)]^{0/-}$. However, the difficulty of lower J_{SC} is remunerated by the V_{OC}, which is the highest among the three complexes, which is 0.66 V.

Using the $[Cu(dmp)_2]^{2+/+}$ redox couple and a mesoporous titania thin-film coated with metal-free organic sensitizer, C218, Peng Wang and his group reported the DSSC device with a PCE of 7% at 100 mW cm^{-2}.[86] The low efficiency of the DSSC device with the copper electrolyte had low electron transfer rates on numerous noble metals, conducting oxides, and carbon black, which resulted in poor fill factor, as evident in their work. The copper device showed 7.8% efficiency when

illuminated with weaker light. This demonstrates the non-linear reliance of photocurrent on the light intensity; further, it can be outlined that the photocurrent under full sunlight would be still imperfect by the mass transport of Cu(II) ions to some extent. When the cell was constructed with the iodine-based electrolyte, they obtained 6.5% PCE, which is lower than that of the copper-based one; the improved efficiency in copper may to credited to the higher V_{OC}, which is improved by 218 mV compared to that of the iodine based one.

In another study, Freitag *et al.* used $[Cu(dmp)_2]^{2+/+}$ with LEG-4, a metal-free organic sensitizer, and achieved high photovoltaic performance of 8.3% with a high V_{OC} of over 1.0 V at 1000 W m^{-2} under AM1.5G conditions.[87] The high voltage is because it requires a driving force of 0.2 V for dye regeneration, which guides to higher efficiencies of the device (Fig. 16). The diffusion coefficient of the copper complexes is high in comparison to that of cobalt redox mediators and hence, the oxidized dye gets reduced faster. In DSSC, the excited dye is quenched by the components of the electrolyte, which affects the efficiency of the device. By using steady state emission measurements and time-correlated single photon counting, we propose that the excited state of the sensitizer quenched by the $[Cu(dmp)_2]^{2+}$ species contributes to electron injection and lowers the overall device accomplishment. These results suggests that the $[Cu\text{-}(dmp)_2]^{2+/+}$ redox couple with the LEG-4 dye has higher recombination when compared to that of the $[Co(bpy)_3]^{3+/2+}$ redox mediator; as a result, multiple recombination pathways such as the reductive quenching of the excited dye and with the TiO_2 layer. Structural modifications of the phenanthroline ligands or the creation of steric hindrance at the dye leads to the minimization of unwanted processes and increase the overall performance of the device.

To further boost the device efficiency using Cu(II/I) redox mediators, particularly using phenanthroline ligands, one has to introduce bulky groups either at the 2nd or 9th positions of the phenanthroline ligand so that the dark current reduces by minimizing the recombination process and leads to higher efficiencies. Colombo *et al.* systematically designed and synthesized three different Cu(II/I) redox mediators, *i.e.*, $[Cu(2,9\text{-dimethyl-}1,10\text{-phenanthroline})_2]PF_6$ $[Cu(dmp)_2]PF_6$, $[Cu(2,9\text{-dimethyl-}4,7\text{-diphenyl-}1,10\text{-phenanthroline})_2]PF_6$ $[Cu(dmpp)_2]PF_6$, and $[Cu(2\text{-mesityl-}4,7\text{-dimethyl-}1,10\text{-phenanthroline})_2]PF_6$, $[Cu(dmmsp)_2]PF_6$.[88] The occurrence of the bulky mesityl group at position 2 but only H at position 9 of phenanthroline causes the steric effect, keeping the mesityl groups on opposite sides of the copper center. The complex $[Cu(dmpp)_2]PF_6$ is involved in outer sphere electron transfer reactions. These consequences, however, could be accomplished only after the meticulous alternative of the dye and suitable TiO_2 passivation approaches, based on the co-adsorption of alkyl-siloxanes. When $[Ru(4,4'\text{-dicarboxy-}2,2'\text{-bipyridine})_2(4,4'\text{-dinonyl-}2,2'\text{-bipyridine})](PF_6)_2$ sensitizer is combined with the copper electrolyte $[Cu(dmmsp)_2]PF_6$ along with the co-mediator Fe(II), it was noticed that the performance of the cell increased with higher J_{SC} values of 4.0 mA cm^{-2} when compared to that of I^-/I_3^-, where it recorded 3.8 mA cm^{-2}. When the $[Ru(4,4'\text{-dicarboxy-}2,2'\text{-bipyridine})_2(4,4'\text{-dinonyl-}2,2'\text{-bipyridine})](PF_6)_2$ dye was combined with the copper complex, attractive advances were revealed compared to that of $[Cu(dmp)_2]PF_6$, where the photocurrent and overall efficiency were doubled. The recovery kinetic studies of Ru(II) showed that the main limitation of these copper complexes was due to slow dye regeneration; however, when the co-mediator was added in the form of 10% polypyridine Fe(II), there was a considerable increase in the photocurrent.

Imahori and co-workers designed and synthesized a series of copper complexes systematically and applied them as redox shuttles for DSSC using the LEG-4 metal-free organic photosensitizer.[89] Although the copper phenanthroline complexes have been reported earlier, they synthesized complexes with substitutions at the 2,9-positions of phenanthroline to check the effect of the ligand structures on the electrochemical and photovoltaic properties. The complexes are $[Cu(bp)_2]^{2+/+}$, (bp = 2-*n*-butyl-1,10-phenanthroline), $[Cu(dmp)_2]^{2+/+}$, (dmp = 2,9-methyl-1,10-phenanthroline), $[Cu(emp)_2]^{2+/+}$, (emp = 2-ethyl-9-methyl-1,10-phenanthroline), $[Cu(dep)_2]^{2+/+}$, (dep = 2,9-diethyl-1,10-phenanthroline), and $[Cu(dpp)_2]^{2+/+}$, (dpp = 2,9-diphenyl-1,10 phenanthroline). When compared to $[Cu(dmp)_2]^{2+/+}$, the complexes $[Cu(emp)_2]^{2+/+}$ and $[Cu(dep)_2]^{2+/+}$ showed more positive redox potentials because of the larger steric hindrance of the ethyl group in the place of the methyl group. But in the case of $[Cu(bp)_2]^{2+/+}$, the redox potential shifts towards the negative direction considerably due to the lower steric hindrance of 2-monosubstituted 1,10-phenanthroline ligands (Fig. 17). The device efficiency of $[Cu(bp)_2]^{2+/+}$ (5.90%) was comparable to that

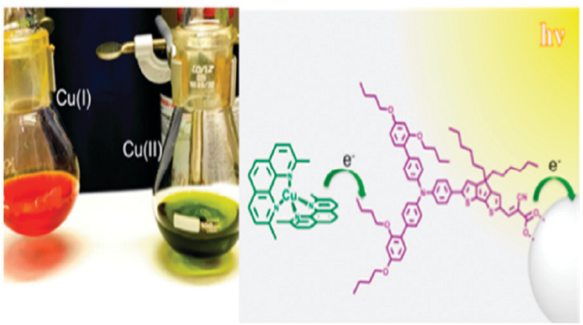

Fig. 16 Pictographic representation of Cu(I) and Cu(II) *in situ* and the structure of the LEG4 sensitizer (ref. 87).

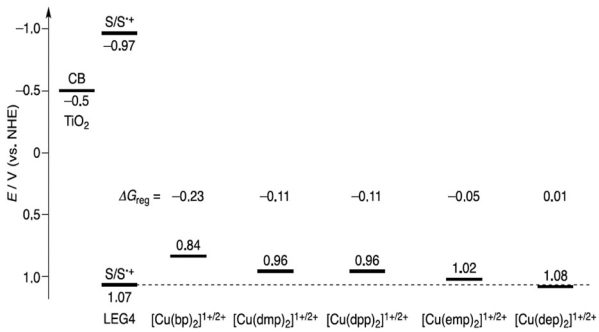

Fig. 17 Energy level diagram comprising of the LEG4 dye with different copper redox couples (ref. 89).

of $[Cu(dmp)_2]^{2+/+}$ (6.29%); strangely, $[Cu(emp)_2]^{+/2+}$ (3.25%), $[Cu(dep)_2]^{2+/+}$ (2.56%), and $[Cu(dpp)_2]^{2+/+}$ (2.21%) showed lower efficiencies. Based on the small ΔGreg of $[Cu(emp)_2]^{+/2+}$ and $[Cu(dep)_2]^{+/2+}$, the lower efficiencies do not seem to be strange at all. It can be argued that the lower efficiency of $[Cu(dpp)_2]^{+/2+}$ relative to $[Cu(dmp)_2]^{+/2+}$ is unexpected since they have the same driving force for dye regeneration. The low efficiencies may be attributed to the sluggish regeneration process, which occurs in microseconds, and the fast charge recombination process. The ligand 2,9-methyl-1,10-phenanthroline is versatile and the copper complex has been used for different sensitizers. For instance, the electrolyte $[Cu(dmp)_2]^{2+/+}$ was used for the metal-free organic dyes of D5, D45, and D35, having different degrees of blocking moieties and the sensitizer D35 with the highest degree of blocking moiety has shown a device efficiency of 9.22%.[70] Further, the device efficiency has risen to 10.3% using Y123 as the sensitizer.[65] Also, the electrolyte $[Cu(dmp)_2]^{2+/+}$ was tested in DSSC devices using porphyrin sensitizers, *i.e.*, LG4 and LG5, but the efficiencies were restricted to 3.98 and 3.30%, respectively.[80]

To mark a sustainable way in both an economic and environment-friendly manner, combined β-substituted Zn^{2+} porphyrin dyes and copper-based electrolytes have been used for DSSCs.[90] Surprisingly, $[Cu(dmsp)_2]^{2+/+}$, a copper electrolyte, attained better performance than $Co^{3+/2+}$ and the I^-/I_3^- allusion electrolyte. In this study, zinc porphyrin having the anchoring group at the β-pyrrole position with three copper complexes was used together as a single cocktail electrolyte, *i.e.*, 2-mesityl-1,10-phenanthroline copper complex (1/2 EI), 2-mesityl-4,7-dimethyl-1-10-phenanthroline copper complex (3/4 EI), and 2,9-dimethyl-1,10-phenanthroline copper complex (5/6 EI). Zn porphyrin is one of the most competent classes of sensitizers in DSSCs and when it coupled with the copper electrolyte system, it was found that its performance was reasonably enhanced. When the D1 sensitizer is coupled with the new copper complex they prepared, it was more efficient because of better diffusion behavior; it showed an amazing 75% enhancement of the PCE with respect to the 5/6 Cu reference. When the electron-releasing methyl groups were removed from the 4 and 7 positions of phenanthroline, they resulted in improved device efficiency because of a very high V_{OC}. Furthermore, because of the more oxidizing $U_{F,redox}$, 1/2-El neatly conquers $[Co(dtb\text{-}bpy)_3]^{3+/2+}$ and the I^-/I_3^- reference couples. It was found that towards D1, the copper complexes were efficient donors; when compared to Co^{2+} and I^-, the dye regeneration was 2-fold to 4-fold increased under equimolar conditions (Fig. 18). Thus, by combining Zn porphyrin with a copper-based electrolyte, they could achieve a better performance in a low-cost and environment-friendly manner.

Due to the lack of an apparent relationship between the electrochemical signatures of the copper complexes and the photoelectrochemical achievement of the solar devices, it is tricky to optimize their coordination sphere. To overcome this drawback and to draw the inherent association between the molecular structural design of these complexes and their electrochemical character, Michele Manca and co-workers synthesized four $Cu^{2+/+}$ electrolytes, *i.e.*, $[Cu(dmsp)_2]PF_6$ complex (1/2 EI), $[Cu(dtp)_2]PF_6$

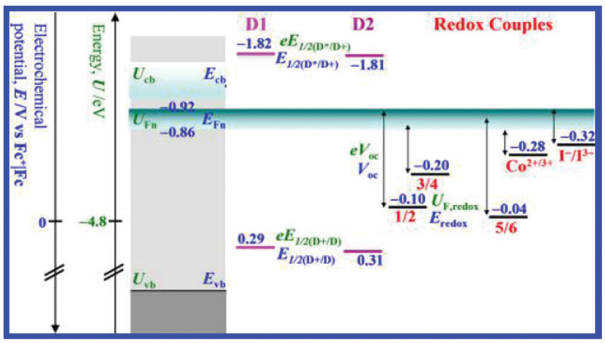

Fig. 18 Schematic representation of the energy levels requisite for cell operation (ref. 90).

complex (3/4 EI), $[Cu(dphp)_2]PF_6$ complex (5/6 EI), and-$[Cu(dnbp)_2]PF_6$ complex (7/8 EI), where the copper center was coordinated by two 1,10-phenanthrolines having a variety of substituents at the 2-position.[91] By electrochemical as well as spectroscopic studies, these complexes were thoroughly studied and these electrolytes were tested in lab-scale devices with two proficient π-extended benzothiadiazole dyes as the sensitizers. It was found that 2-aryl-1,10-phenanthrolines effectively coalesce the appropriate electrochemical and optical properties. In order to optimize the DSSC, mass transport, most favorable balance between dye regeneration capability, and heterogeneous electron transfer at both the counter electrode and at the TiO_2 interface should be attained, even though fast electron transfer kinetics commonly affects the dye regeneration process positively (Fig. 19). In the series of complexes they prepared, $[Cu(dtp)_2]^{2+/+}$ obtained a better efficiency of 20 and 15% using $[Co(bpy)_3]^{3+/2+}$(bpy = 2,2′-bipyridine) and I^-/I_3^- electrolytes, respectively.

With homoleptic complexes of 2-substituted-1,10- phenanthrolines, four Cu^{2+}/Cu^+ redox couples were synthesized and their optical and electrochemical properties could be modulated by the functionalization of the positions adjoining the N atoms.[92] Hence, by combining cyclic voltammetry and visible absorption spectroscopy, it was shown that the copper-based redox couples be produced with important characteristics in DSSC by the asymmetric substitution of ligands. The intensity of the MLCT bands decreased in the 2-substituted ligands, in

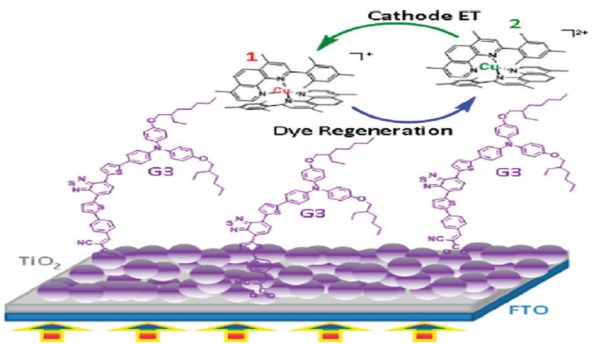

Fig. 19 Mode of binding of the G3 sensitizer on nanocrystalline TiO_2 and the dye regeneration process from the redox couple to the dye (ref. 91).

particular, the associated Cu(I) coordination compounds, which resembles the already known effect of asymmetry observed in the exterior 4 and 7 positions of phenanthrolines. When aryl groups are preferred over alkyl groups, this effect is enhanced. $E_{1/2}$ and k_{heter} were found to be indirectly proportional through electrochemical studies but are affected by the geometry of the complex and its flexibility, which are adapted by the rotational freedom of the internal substituents and not only by steric hindrance. Optimal optical and electrochemical properties are effectively combined because of 2-aryl derivatives; in short circuit conditions, quantitative dye regeneration efficiencies are achieved, which is credited to the better positive oxidation potentials, lower molecular extinction coefficient, and well-balanced electron transfer kinetics. 3/4-El clearly shows different power conversion efficiencies of 15 and 20% for the iodide/triiodide redox shuttle and the $[Co(bpy)_3]^{3+/2+}$ redox shuttle, respectively, when formulated at similar concentrations; this efficiency overcame the result of their previous 1/2-El copper mediation due to the positive half-wave potential.

The Cu(I) complex-based sensitizer and its use in DSSC with the $Cu^{2+/+}$ redox couple is interesting. Alessia Colombo and group synthesized and thoroughly characterized two novel heteroleptic copper (1) sensitizers having 6,6′dimethyl-2,2′-bipyridine-4,4′-dibenzoic acid to anchor the dye on the titania surface and a π-delocalized 2-(*R*-phenyl)-1*H*-phenanthro[9,10-*d*]imidazole (R = NPh_2 or *O*-hexyl) ancillary ligand.[93,94] Since they are similar complexes having 2,9-dimesityl-1,10-phenanthroline as the ancillary ligand, their performance in the DSSCs as dyes were much similar when homoleptic copper complexes or iodide/triiodide electrolytes were used. However, in full copper complexes, it was found to have better potential from both the experimental results and theoretical calculations. Since the compounds prepared are similar, possessing 2,9-dimesityl-1,10-phenanthroline as an ancillary ligand, they could be coupled with the iodide/triiodide electrolyte to prepare a DSSC with moderate efficiency. Based on the electron shuttle, they can also be coupled with the homoleptic copper electrolyte to provide full-copper DSSCs with adequate to good performance. It was noticed that in copper dyes, the use of π-delocalized ancillary ligands was done for electron transfer augmentation from the electrolyte to the dye and directionality for electron injection into the TiO_2 conduction band and was not adequate to enhance light harvesting drastically. The main absorption was assigned to be MLL′CT from the TDDFT calculations, in which phenanthroline was also involved and not only the bipyridyl ligand, which upon TiO_2 sensitization should point in the opposite direction of the TiO_2 surface. Due to phenanthroline participation, there was a reduction in the charge transfer directionality, in which the excited state originating visible light absorption therefore becomes detrimental. To avoid interference with the low-lying MLCT transitions, this class of compounds should be tuned to up-shift the phenanthroline-based LUMOs by electron-donating ligands. Keeping earth-abundant components in mind, this study shows copper complexes with potential applications in DSSCs (Table 2).

Lennert *et al.* designed and synthesized a series of phenanthroline-based homoleptic and heteroleptic Cu(II/I) redox shuttles, which were tested in a DSSC using the D35 organic dye.[95] Initially, from a homoleptic copper complex containing bathocuproine ligands, $[Cu(bcp)_2]OTf$ (bcp = 2,9-dimethyl-4,7-diphenyl-1,10-phenanthroine) and $[[Cu(bcp)_2]]$, one of them was substituted by another N- or P-coordinating ligand. They are [Cu(bcp)(tmp)]OTf, [Cu(bcp)(dppm)]OTf (dppm = (diphenylphosphino)methane), [Cu(bcp)(dppx)]OTf (dppx = 4,5-bis(diphenylphosphino)-9,9-dimethylxanthene) and $[Cu(dmp)_2]OTf$. The absorption and redox properties of these complexes are very attractive for DSSC applications. The electrochemical properties of P-containing ligands, *i.e.*, complex D and E, were not stable. Electrochemical impedance studies suggest that the A and E homoleptic complexes have the highest diffusion coefficients and the maximum current density. For B, C, and D heteroleptic complexes, it was found that the performance depended on the size of the appropriate ligand. Also, it has been noticed in heteroleptic complexes charge transport resistance exceeds 200 Ω, whereas a reasonably low transport resistance of 100 Ω is obtained for homoleptic complexes. The change in the efficiency was dependent on lesser resistance against the recombination of A relative with reference E; homoleptic complexes obtained the best PCE in terms of DSSC. With and without copper complexes, the complementary transient absorption studies showed start effects, charge injection, long lived fingerprints of dye cation, as well as geminate recombination and non-recombination. Marked variations were noticed in terms of long-lived fingerprints of the one-electron oxidized form of D35 when the electrolyte was present, which implied better dye regeneration. The geminate and non-geminate recombination processes, in the presence of the electrolyte, were largely unaffected.

3.3 Tetradentate ligands

In addition to bidentate and tridentate polypyridyl ligands that include both bipyridine and phenanthroline, there are other ligands having either P or O as the coordinating atoms or those that are beyond tridentate ligands, *i.e.*, tetradentate ligands, in which all the four coordination sites in a ligand molecule considerably decrease the geometry rearrangements (Fig. 20). Freitag and co-workers have designed and synthesized a $Cu(oxabpy)^{2+/+}TFSI_{1/2}$ (oxabpy = 6,6′-bis(4-(*S*)-isopropyl-2-oxazolinyl)-2,2′-bipyridine) for DSSC application using Y123 as the photosensitizer.[96] In this complex, copper was present in the square planar geometry; it possesses low reorganizational energies and in turn has smaller losses of photovoltage. Exceptionally long electron lifetime was achieved due to sluggish recombination kinetics of the excited electron between TiO_2 and the Cu(II) species. 6.2% of PCE was obtained with a high photovoltage of 920 mV and photocurrents of 1 0 mA cm^{-2}. Despite the square planar complex obtained in a highly viscous gel, the charge transport performance obtained with Cu(oxabpy) was comparable with that of the previously reported $Cu(tmby)_2^{2+/+}$ redox mediator. The improvement in charge transport in the

Table 2 Photovoltaic data of copper(II/I) redox shuttles using phenanthroline ligands

Electrolyte	Dye	J_{SC}[a]	V_{OC}[a]	FF[a]	η (%)	Ref.
$[Cu(dmp)_2]^{2+/+}$	N719	3.2	0.79	0.55	1.4	47
$[Cu(phen)_2]^{2+/+}$	N719	0.48	0.57	0.43	0.12	47
$[Cu(dmp)_2]^{2+/+}$	C218	11.29	0.93	0.66	7.0	86
$[Cu(dmp)_2]^{2+/+}$	LEG4	12.6	1.02	0.62	8.3	87
$[Cu(dmp)_2]PF_6$	$[Ru(dcbpy)_2(dnbpy)](PF6)_2$	1.10	0.73	0.50	0.4	88
$[Cu(dmp)_2]PF_6$	$[Ru(dcbpy)_2(dnbpy)](PF6)_2$	1.10	0.71	0.49	0.4	88
$[Cu(dmpp)_2]PF_6$	$[Ru(dcbpy)_2(dnbpy)](PF6)_2$	1.10	0.71	0.49	0.4	88
$[Cu(dmmsp)_2]PF_6$	$[Ru(dcbpy)_2(dnbpy)](PF6)_2$	2.4	0.58	0.58	0.9	88
$[Cu(dmmsp)_2]PF_6$	$[Ru(dcbpy)_2(dnbpy)](PF6)_2$	2.0	0.60	0.64	0.9	88
$[Cu(bp)_2]^{2+/+}$	LEG4	10.60	0.84	0.66	5.90	89
$[Cu(dmp)_2]^{2+/+}$	LEG4	10.0	1.03	0.61	6.29	89
$[Cu(emp)_2]^{2+/+}$	LEG4	7.52	0.82	0.53	3.25	89
$[Cu(dep)_2]^{2+/+}$	LEG4	6.77	0.81	0.46	2.56	89
$[Cu(dpp)_2]^{2+/+}$	LEG4	4.18	0.85	0.62	2.21	89
$[Cu(dmp)_2]^{2+/+}$	D5	9.02	1.13	0.74	7.53	70
$[Cu(dmp)_2]^{2+/+}$	D45	9.90	1.02	0.74	7.48	70
$[Cu(dmp)_2]^{2+/+}$	D35	11.40	1.14	0.71	9.22	70
$[Cu(dmp)_2]^{2+/+}$	LG4	6.89	0.89	0.65	3.98	80
$[Cu(dmp)_2]^{2+/+}$	LG5	5.06	0.86	0.69	3.30	80
$[Cu(dmp)_2]^{2+/+}$	Y123	13.60	1.06	0.69	10.3	65
$[Cu(dmsp)_2]^{2+/+}$	D1	5.9	0.81	0.77	3.9	90
$[Cu(dmmsp)_2]^{2+/+}$	D1	5.6	0.68	0.77	2.9	90
$[Cu(dmp)_2]^{2+/+}$	D1	3.5	0.86	0.70	2.1	90
$[Cu(dmsp)_2]^{2+/+}$	D2	4.80	0.75	0.74	2.7	90
$[Cu(dmp)_2]^{2+/+}$	G3	3.8	0.86	0.53	1.9	91
$[Cu(dmsp)_2]^{2+/+}$	G3	11.4	0.83	0.59	5.6	91
$[Cu(dtp)_2]^{2+/+}$	G3	11.1	0.87	0.62	6.0	91
$[Cu(dphp)_2]PF_6$	G3	8.0	0.88	0.69	4.9	91
$[Cu(dnbp)_2]^{2+/+}$	G3	10.1	0.86	0.66	5.7	91
$[Cu(dmsp)_2]^{2+/+}$	G4	11.7	0.84	0.54	5.3	91
$[Cu(dtp)_2]^{2+/+}$	G4	11.1	0.87	0.62	6.0	91
$[Cu(dphp)_2]PF_6$	G4	10.2	0.81	0.58	4.8	90
$[Cu(dnbp)_2]^{2+/+}$	G4	10.1	0.78	0.66	5.7	90
$[Cu(dmp)_2]^{+}/[Cu(dmp)_2Cl]^{+}$	D3	0.9	037	0.37	0.1	92
$[Cu(dnbp)_2]^{2+/+}$	D1	3.8	0.59	0.61	1.4	92
$[Cu(n\text{-butyl-dmp})_2]^{2+/+}$	D2	3.2	0.57	0.67	1.2	94
$[Cu(dnbp)_2]^{2+/+}$	D3	2.8	0.57	0.62	1.1	94
Copper electrolyte	D35	5.47	0.84	0.47	2.14	95

[a] Error limits: J_{SC} = ±0.20 mA cm^{-2}, V_{OC} = ±0.30 mV, FF = ±0.03, and η = ±0.1.

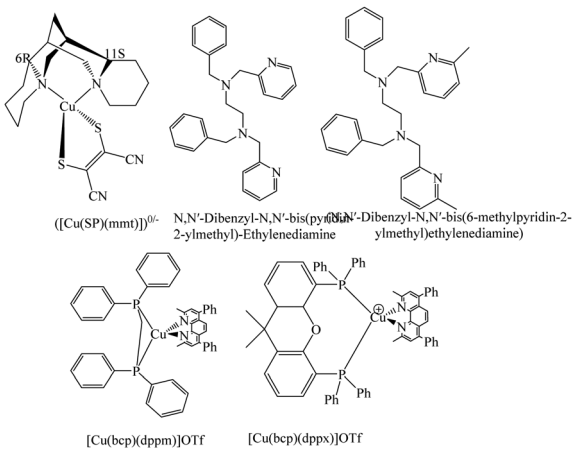

Fig. 20 Molecular structure of tetradentate ligands.

gel-like electrolyte originates from charge hopping mechanism on top of diffusive transport.

Rodrigues *et al.* have designed and synthesized three copper complexes featuring tetradentate ligands and they are $[Cu(bpyph)_2]^{2+/+}$ (bpyph = 2,2′-di([2,2′-bipyridin]-6-yl)-1,10-biphenyl), $[Cu(mbptb)_2]^{2+/+}$ (mbptb = 2,2′-bis(methyltriazole-pyridine)-biphenyl), and $[Cu(mcptb)_2]^{2+/+}$ (mcptb = 2,2′-bis(methyltriazole-4-trifluoromethyl-pyridine)-biphenyl).[97] All these three tetradentated copper complexes were evaluated in DSSCs using Y123 as the photosensitizer and their performance was compared with $[Cu(bpye)_2]^{2+/+}$. To improve the power conversion efficiency, a new strategy has been adopted by introducing neutral polyaromatic ligands with partial flexibility, thereby reducing the voltage losses affiliated to the redox couple. Quantum mechanical calculations were used for inner-sphere electron transfer reorganization energies (λ) calculations and evaluated for the commonly used $[Co(bpy)_3]^{3+/2+}$ complex, which has a reported λ of 0.61 eV. The triazole group in $[Cu(mbptb)_2]^{+/2+}$ and $[Cu(mcptb)_2]^{2+/+}$ shows a slight increase in the reorganization energies but when compared to the traditional copper bidentate complexes, their reorganizational energies are lower. The lower reorganizational energies (0.34–053 eV) of the tetradenate copper complexes are due to geometrical constraints and their activation with low driving forces for dye regeneration. Because of this, it allows better efficient electron transfer reactions, primarily to enhance the J_{SC}. By using the PEDOT counter electrode

Table 3 Photovoltaic data of copper(I/II) redox shuttles using tetradenate ligands

Electrolyte	Dye	J_{SC}[a]	V_{OC}[a]	FF[a]	η (%)	Ref.
$[Cu(SP)(mmt)]^{0/-}$	N719	4.4	0.66	0.44	1.3	47
$[Cu(oxabpy)]^{2+/+}$	Y123	9.75	0.92	0.69	6.2	96
		1.32	0.86	0.79	8.9	
$[Cu(bpyph)_2]^{2+/+}$	Y123	5.7	0.69	0.77	3.1	97
$[Cu(mbptb)_2]^{2+/+}$	Y123	10.2	0.69	0.72	4.7	97
$[Cu(mcptb)_2]^{2+/+}$	Y123	7.9	0.79	0.75	4.3	97
(*N*,*N*′-Dibenzyl-*N*,*N*′-bis(6-methylpyridin-2-ylmethyl)ethylenediamine)(ligand)	Y123	15.6	0.87	0.68	9.2	98

[a] Error limits: J_{SC} = ±0.20 mA cm^{-2}, V_{OC} = ±0.30 mV, FF = ±0.03, and η = ±0.1.

with the $[Cu(mbptb)_2]^{+/2+}$ redox shuttle, a PCE of 4.7% was achieved, whereas with the Pt counter electrode, a PCE of 4.4% was observed (Table 3).

The efficiencies obtained by tetradenate copper complexes are not sufficient to commercialize the technology. To further enhance the PCE of tetradenate copper complexes, Hu *et al.* designed and synthesized two complexes, namely, $[Cu(dadp)_2]^{2+/+}$ (dadp = *N*,*N*′-dibenzyl-*N*,*N*′-bis-(pyridin-2-ylmethyl)ethylenediamine) and $[Cu(dmdp)_2]^{2+/+}$ (dmdp = *N*,*N*′-dibenzyl-*N*,*N*′-bis-(pyridin-2-ylmethyl)ethylenediamine).[98] The redox potential of $[Cu(dmdp)_2]^{2+/+}$ shifts positively by 300 mV due to the introduction of the methyl group because of the steric-hindrance effect of L2, which manages a 180 mV increase in the V_{OC}. In addition to this, the methyl group on the tetradentate ligand diminishes the internal reorganization energy that increases the high dye regeneration yield and as a result, an improved PCE of 9.2% is achieved. More importantly, the complexes have good air, photo, and electrochemical stability, thus resulting in longer durability of the whole DSSC. The present study for the sensible design of the coordination sphere of the copper complexes as an efficient tactic to tune the redox potentials of the redox couple can help to design redox couples in the future.

A majority of oxidation potentials of Cu complexes are more positive and the dyes having higher oxidation potentials are suitable combination for DSSC applications. In general, such type of oxidation potentials can be easily tuned by metal-free organic dyes as well as pigment-based dyes (porphyrins, phthalocyaines, corroles *etc.*), which are more compatible with the Cu(II/I) redox couples. In addition to this, the Cu complexes have higher diffusion coefficients compared to the Co-based alternatives. Therefore, the Cu-based systems are considered to exhibit less mass transport limitations compared to Co-based systems and show better device efficiency under low-light conditions.

4. Conclusions

In conclusion, the redox shuttle dictates the efficiency and durability of the device. Though the certified efficiencies have crossed 11% using the traditional I^-/I_3^- redox mediator, their module development is hindered mainly due to its volatile nature and complementary absorption with the sensitizer. To conquer these boundaries, several attempts have been dedicated towards alternative redox shuttles for the past couple of decades, particularly transition metals having variable oxidation states. By tuning redox potential of the redox shuttle will help in controlling the overpotential that ultimately leads to improving the efficiency of the device. Co(II/III) redox mediators using polypyridyl ligands have successfully tuned the redox potential to suit various sensitizers and have achieved an device efficiency of more than 14% recently. However, a major bottleneck for Co(II/III) redox shuttles is the mass transport and the health hazards, which hamper the commercialization of the technology. Inspired from biological electron transport systems that involve copper complexes, Cu(II/I) redox shuttles might be the alternative choice as redox mediators for DSSC applications. The main advantage of the Cu(II/I) redox shuttles is that their redox potentials are more positive than that of Co(III/II) so that the regeneration potential of the oxidized dye is ~0.1 V. This will not only control the recombination of the oxidized dye with electrons in the TiO_2 conduction band but also improve the V_{OC} of the device. Another drawback in Co(III/II) redox mediators is mass transport due to bulky nature, which is remarkable at high incident light intensities and reduces the overall device accomplishments. Several sensitizers using Cu(II/I) redox mediators have crossed the device efficiency of 10% under 1 sun irradiation and in the case of co-sensitization, the device efficiency has even crossed 13%. Similar to that in Co(III/II) redox mediators, copper mediators also suffer from mass transport; however, in the case of Cu(II/I) redox mediators, particularly in the co-sensitization of metal-free organic dyes, it has reached 31.8% at 1000 lux intensity. Also, in one of the bipyridyl copper complexes using organic dye, a better efficiency of 11% in the solid state has been obtained rather than that in the liquid state. All these results are encouraging to researchers interested in copper electrolytes under low light conditions, which have potential for the commercialization of technology, precisely for Internet of Things (IoT) applications.

Conflicts of interest

There are no conflicts to declare.

Acknowledgements

The authors would like to thank Department of Science and Technology, Indo-Israel bilateral programme for financial support. K. S. V. and S. P. thanks to DST for Inspire Fellowship and DST-Inspire Faculty (DST/INSPIRE/04/2015/001457). The authors thank the Director, CSIR-IICT (Manuscript No. IICT/Pubs./2020/349).

Notes and references

1 M. Nicole, B. Matteo, F. Lucia, B. Nadia, G. Claudio, B. Federico and B. Claudia, *Green Chem.*, 2020, **22**, 7168–7218.
2 A. M. Hisham, B. Vikas and K. B. Sanjay, *Renewable Sustainable Energy Rev.*, 2020, **121**, 109678.
3 M. Mrinalini, N. Islavath, S. Prasanthkumar and L. Giribabu, *Chem. Rec.*, 2019, **19**, 661–674.
4 G. Jiawei, K. Sumathy, Q. Qiquano and Z. Zhengping, *Renewable Sustainable Energy Rev.*, 2017, **68**, 234–246.
5 L. Giribabu, R. K. Kanaparthi and V. Velkannan, *Chem. Rec.*, 2012, **12**, 306–328.
6 S. Mozaffari, M. R. Nateghi and M. B. Zarandi, *Renewable Sustainable Energy Rev.*, 2017, **71**, 675–686.
7 N. H. Reich, W. G. J. H. M. van Sark, E. A. Alsema, R. W. Lof, R. E. I. Schropp, W. C. Sinke and W. C. Turkenburg, *Sol. Energy Mater. Sol. Cells*, 2009, **93**, 1471–1481.
8 B. O'Regan and M. Grätzel, *Nature*, 1991, **353**, 737–740.
9 K. Kakiage, Y. Aoyama, T. Yano, K. Oya, J.-I. Fujisawa and M. Hanaya, *Chem. Commun.*, 2015, **51**, 15894–15897.
10 www.nrel.gov/pv, National Renewable Energy Laboratory (NREL).
11 S. Mathew, A. Yella, P. Gao, R. Humphry-Baker, B. F. E. Curchod, N. A. Astani, I. Tavernelli, U. Rothlisberger, M. K. Nazeeruddin and M. Gratzel, *Nat. Chem.*, 2014, **6**, 242–247.
12 J. Wu, Z. Lan, J. Lin, M. Huang, Y. Huang, L. Fan and G. Luo, *Chem. Rev.*, 2015, **115**, 2136–2173.
13 A. Mohammad, *J. Eng. Chem.*, 2015, **24**, 686–692.
14 N. C. D. Nath and J.-J. Lee, *J. Ind. Eng. Chem.*, 2019, **78**, 53–65.
15 L. Giribabu, R. Bolligarla and M. Panigrahi, *Chem. Rec.*, 2015, **15**, 760–788.
16 J. W. Ondersma and T. W. Hamann, *Coord. Chem. Rev.*, 2013, **257**, 1533–1543.
17 T. W. Hamann, O. K. Farah and J. T. Hupp, *J. Phys. Chem. C*, 2008, **112**, 19756–19764.
18 M. Wang, C. Grätzel, S. M. Zakeeruddin and M. Grätzel, *Energy Environ. Sci.*, 2012, **5**, 9394–9405.
19 P. J. Cameron, L. M. Peter, S. M. Zakeeruddin and M. Grätzel, *Coord. Chem. Rev.*, 2004, **284**, 1447–1453.
20 G. Boschloo and A. Hegfeldt, *Acc. Chem. Res.*, 2009, **42**, 1819–1826.
21 H. Kusama, *J. Photochem. Photobiol., A*, 2019, **376**, 255–262.
22 V. Chakrapani, D. Baker and P. V. Kamat, *J. Am. Chem. Soc.*, 2011, **133**, 9607–9615.
23 C. Teng, X. Yang, C. Yuan, C. Li, R. Chen, H. Tian, S. Li, A. Hagfeldt and L. Sun, *Org. Lett.*, 2009, **11**, 5542–5545.
24 Z.-S. Wang, K. Sayama and H. Sugihara, *J. Phys. Chem. B*, 2005, **109**, 22449–22455.
25 B. V. Bergeron, A. Marton, G. Oskam and G. J. Meyer, *J. Phys. Chem. B*, 2005, **109**, 937–943.
26 F. Pichot and B. A. Gregg, *J. Phys. Chem. B*, 1999, **104**, 6–10.
27 Z. Yu, S. You, C. Wang, C. Bu, S. Bai, Z. Zhou, Q. Tai, W. Liu, S. Guo and X. Zhao, *J. Mater. Chem. A*, 2014, **2**, 9007–9010.
28 Y. Zhang, Z. Sun, C. Shi and F. Yan, *RSC Adv.*, 2016, **6**, 70460–70467.
29 W. Zhang, L. Qiu, X. Chen and F. Yan, *Electrochim. Acta*, 2014, **117**, 48–54.
30 M. Cheng, X. Yang, F. Zhang, J. Zhao and L. Sun, *Angew. Chem., Int. Ed.*, 2012, **51**, 9896–9899.
31 H. Iftikhar, G. G. Sonai, S. G. Hashmi, A. F. Nogueira and P. D. Lund, *Materials*, 2019, **12**, 1998.
32 Y. Liu, S.-C. Yiu, C.-L. Ho and W.-Y. Wong, *Coord. Chem. Rev.*, 2018, **375**, 514–557.
33 S. Carli, E. Benazzi, L. Casarin, T. Bernardi, V. Bertolasi, R. Argazzi, S. Caramoria and C. A. Bignozzi, *Phys. Chem. Chem. Phys.*, 2016, **18**, 5949–5956.
34 F. Bella, S. Galliano, G. Gerbaldi and G. Viscardi, *Energies*, 2016, **9**, 384.
35 A. Apostolopoulou, M. Vlasiou, P. A. Tziouris, C. Tsiafoulis, A. C. Tsipis, D. Rehder, T. A. Kabanos, A. D. Keramidas and E. Stathatos, *Inorg. Chem.*, 2015, **54**, 3979–3988.
36 H. Tian and L. Sun, *J. Mater. Chem.*, 2011, **21**, 10592–10601.
37 T. Li, A. M. Spokoyny, C. She, O. K. Farha, C. A. Mirkin, T. J. Marks and J. T. Hupp, *J. Am. Chem. Soc.*, 2010, **132**, 4580–4582.
38 S. C. Pradhan, A. Hegfeldt and S. Soman, *J. Mater. Chem. A*, 2018, **6**, 22204–22214.
39 K. Kakiage, Y. Aoyama, T. Yano, K. Oya, J.-I. Fujisawa and M. Hanaya, *Chem. Commun.*, 2015, **51**, 15894–15897.
40 S. Mathew, A. Yella, P. Gao, R. Humphry-Baker, B. F. E. Curchod, N. Ashari-Astani, I. Tavernelli, U. Rothlisberger, M. K. Nazeeruddin and M. Grätzel, *Nat. Chem.*, 2014, **6**, 242–247.
41 B. Pashaei, H. Shahroosvand and P. Abbasi, *RSC Adv.*, 2015, **5**, 94814–94848.
42 L. Leyssens, B. Vinck, C. VanderStraeten, F. Wuyts and L. Maes, *Toxicology*, 2017, **387**, 43–56.
43 J. Fritzsche, C. Borisch and Ch Schaefer, *Clin. Orthop. Relat. Res.*, 2012, **470**, 2325–2331.
44 D. V. Brusselen, T. K. Kitenge, S. Mbuyi-Musanzayi, T. L. Kasole, L. K. Ngombe, P. M. Obadia, D. K. Wa Mukoma, K. V. Herck, D. Avonts, K. Devriendt, E. Smolders, C. B. L. Nkulu and B. Nemery, *Lancet Planet. Health*, 2020, **4**, e158–e167.
45 L. Giribabu, T. Bessho, M. Srinivasu, Ch. V. Kumar, Y. Soujanya, V. G. Reddy, P. Y. Reddy, J.-H. Hum, M. Grätzel and M. K. Nazeeruddin, *Dalton Trans.*, 2011, **40**, 4497–4504.
46 L. Giribabu, Ch. V. Kumar, Ch. S. Rao, V. G. Reddy, P. Y. Reddy, M. Chandrasekharam and Y. Soujanya, *Energy Environ. Sci.*, 2009, **2**, 770–773.
47 S. Hattori, Y. Wada, S. Yanagida and S. Fukuzumi, *J. Am. Chem. Soc.*, 2005, **127**, 9648–9654.
48 E. L. Gross, *Photosynth. Res.*, 1993, **37**, 103–116.
49 A. G. Sykes, *Adv. Inorg. Chem.*, 1991, **107**, 377–408.
50 C. M. Groeneveld, S. Dahlin, B. Reinhammar and G. W. Canters, *J. Am. Chem. Soc.*, 1987, **109**, 3247–3250.
51 R. A. Marcus and H. Eyring, *Annu. Rev. Phys. Chem.*, 1964, **15**, 155–196.

52 A. R. Marcus and N. Sutin, *Biochim. Biophys. Acta*, 1985, **811**, 265–322.
53 D. B. Rorabacher, *Chem. Rev.*, 2004, **104**, 651–698.
54 B. J. Hathaway, *Coord. Chem. Rev.*, 1981, **35**, 211–252.
55 B. J. Hathaway and D. E. Billing, *Coord. Chem. Rev.*, 1970, **5**, 143–207.
56 J. M. Guss, H. D. Bartunik and H. C. Freeman, *Acta Crystallogr., Sect. B: Struct. Sci.*, 1992, **48**, 790–811.
57 E. T. Adman, *Adv. Protein Chem.*, 1991, **42**, 145–197.
58 E. I. Solmon and R. G. Hadt, *Coord. Chem. Rev.*, 2011, **255**, 774–789.
59 E. I. Solmon, R. K. Szilgyi, S. D. George and L. Basumallick, *Chem. Rev.*, 2004, **104**, 419–458.
60 E. I. Solmon, L. B. LaCorix and D. W. Randal, *Pure Appl. Chem.*, 1998, **70**, 799–808.
61 L. B. LaCroix, S. E. Shadle, Y. Wang, B. A. Averill, B. Hedman, K. O. Hodgson and E. I. Solmon, *J. Am. Chem. Soc.*, 1996, **118**, 7755–7768.
62 F. Balu, *Monatsh. Chem.*, 1889, **10**, 375–388.
63 M. Brugnati, S. Caramori, S. Cazzanti, L. Marchini, R. Argazzi and C. A. Bignozzi, *Int. J. Photo Eng.*, 2007, 80756.
64 J. Cong, D. Kinschel, Q. Daniel, M. Safdar, E. Gabrielsson, H. Chen, P. H. Svensson, L. Sunce and L. Kloo, *J. Mater. Chem. A*, 2016, **4**, 14550–14554.
65 Y. Saygili, M. Söderberg, N. Pellet, F. Giordano, Y. Cao, A. B. Muñoz-García, S. M. Zakeeruddin, N. Vlachopoulos, M. Pavone, G. Boschloo, L. Kavan, J.-E. Moser, M. Grätzel, A. Hagfeldt and M. Freitag, *J. Am. Chem. Soc.*, 2016, **138**, 15087–15096.
66 J. Li, X. Yang, Z. Yu, G. G. Gurzadyan, M. Cheng, F. Zhang, J. Cong, W. Wang, H. Wang, X. Li, L. Kloo, M. Wang and L. Sun, *RSC Adv.*, 2017, **7**, 4611–4615.
67 J. V. S. Krishna, D. Koteshwar, T. H. Chowdhury, S. P. Singh, I. Bedja, A. Islam and L. Giribabu, *J. Mater. Chem. C*, 2019, **7**, 13594–13605.
68 N. V. Krishna, J. V. S. Krishna, S. P. Singh, L. Giribabu, L. Han, I. Bedja, R. K. Gupta and A. Islam, *J. Phys. Chem. C*, 2017, **121**, 6464–6477.
69 Y. Wang and T. W. Hamann, *Chem. Commun.*, 2018, **54**, 12361–12364.
70 Y. Saygili, M. Stojanovic, H. Michaels, J. Tiepelt, J. Teuscher, A. Massaro, M. Pavone, F. Giordano, S. M. Zakeeruddin, G. Boschloo, J.-E. Moser, M. Grätzel, A. B. Muñoz-García, A. Hagfeldt and M. Freitag, *ACS Appl. Energy Mater.*, 2018, **1**, 4950–4962.
71 L. Kavan, Y. Saygili, M. Freitag, S. M. Zakeeruddin, A. Hagfeldt and M. Grätzel, *Electrochim. Acta*, 2017, **227**, 194–202.
72 P. Ferdowsi, Y. Saygili, S. M. Zakeeruddin, J. Mokhtari, M. Grätzel, A. Hagfeldt and L. Kavan, *Electrochim. Acta*, 2018, **265**, 194–201.
73 H. Jiang, Y. Ren, W. Zhang, Y. Wu, E. C. Socie, B. I. Carlse, J.-E. Moser, H. Tian, S. M. Zakeeruddin, W.-H. Zhu and M. Grätzel, *Angew. Chem., Int. Ed.*, 2020, **59**, 9324–9329.
74 M. Freitag, J. Teuscher, Y. Saygili, X. Zhang, F. Giordano, P. Liska, J. Hua, S. M. Zakeeruddin, J.-E. Moser, M. Grätzel and A. Hagfeldt, *Nat. Photonics*, 2017, **11**, 372–378.
75 E. Tanaka, H. Michaels, M. Freitag and N. Robertson, *J. Mater. Chem. A*, 2020, **8**, 1279–1287.
76 Y. Cao, Y. Liu, S. M. Zakeeruddin, A. Hagfeldt and M. Grätzel, *Joule*, 2018, **2**, 1108–1117.
77 Y. Cao, Y. Saygili, A. Ummadisingu, J. Teuscher, J. Luo, N. Pellet, F. Giordano, S. M. Zakeeruddin, J.-E. Moser, M. Freitag, A. Hegfeldt and M. Grätzel, *Nat. Commun.*, 2017, **8**, 15390.
78 M. Freitag, Q. Daniel, M. Pazoki, K. Sveinbjörnsson, J. Zhang, L. Sun, A. Hagfeldt and G. Boschloo, *Energy Environ. Sci.*, 2015, **8**, 2634–2637.
79 A. Glinka, M. Gierszewski, B. Gierczyk, G. Burdziński, H. Michaels, M. Freitag and M. Ziółek, *J. Phys. Chem. C*, 2020, **124**, 2895–2906.
80 T. Higashino, H. Liyama, I. Nishimura and H. Imahori, *Chem. Lett.*, 2020, **49**, 936–939.
81 G. Wilkinson, R. D. Gillard and J. A. M. Cleverty, *Comprehensive Coordination Chemistry*, Pergamon, Oxford, UK, vol. 2, 1987.
82 T. Hiroshama, Y. Kuranuki, E. Ebina, T. Sugizaki, H. Arii, M. Chikira, P. T. Selvi and M. Palaniandavar, *J. Inorg. Biochem.*, 2005, **99**, 1205–1219.
83 Z. M. Wang, H. K. Lin, M. Xu, T. F. Liu, S. R. Zhu and Y. T. Chen, *Bioorg. Med. Chem.*, 2001, **9**, 2849–2855.
84 A. Y. Kovalevsky, M. Gembicky and P. Coppens, *Inorg. Chem.*, 2004, **43**, 8282–8289.
85 B. W. Marcus and D. R. McMillan, *Inorg. Chem.*, 1980, **19**, 3519–3522.
86 Y. Bai, Q. Yu, N. Cai, Y. Wang and P. Wang, *Chem. Commun.*, 2011, **47**, 4376–4378.
87 M. Freitag, F. Giordano, W. Yang, M. Pazoki, Y. Hao, B. Zietz, M. Grätzel, A. Hagfeldt and G. Boschloo, *J. Phys. Chem. C*, 2016, **120**, 9595–9603.
88 A. Colombo, C. Dragonetti, M. Magni, D. Roberto, F. Demartin, S. Caramori and C. A. Bignozzi, *ACS Appl. Mater. Interfaces*, 2014, **6**, 13945–13955.
89 T. Higashino, H. Liyama, S. Nimura, Y. Kurumisawa and H. Imahori, *Inorg. Chem.*, 2020, **59**, 452–459.
90 A. Colombo, G. Di Cardo, C. Dragonetti, M. Magni, A. O. Biroli, M. Pizzotti, D. Roberto, F. Tessore, E. Benazzi, C. A. Bignozzi, L. Casarin and S. Caramori, *Inorg. Chem.*, 2017, **56**, 14189–14197.
91 M. Magni, R. Giannuzzi, A. Colombo, M. P. Cipolla, C. Dragonetti, S. Caramori, S. Carli, R. Grisorio, G. P. Suranna, C. A. Bignozzi, D. Roberto and M. Manca, *Inorg. Chem.*, 2016, **55**, 5245–5253.
92 E. Benazzi, M. Magni, A. Colombo, C. Dragonetti, S. Caramori, C. A. Bignozzi, R. Grisorio, G. P. Suranna, M. P. Cipolla, M. Manca and D. Roberto, *Electrochim. Acta*, 2018, **271**, 180–189.
93 A. Colombo, C. Dragonetti, F. Fragnani, D. Roberto, F. Melchiorre and P. Biagini, *Dalton Trans.*, 2019, **48**, 9818–9823.

94 C. Dragonetti, M. Margni, A. Colombo, F. Fagnani, D. Roberto, F. Melchiorre, P. Biagini and S. Fantacci, *Dalton Trans.*, 2019, **49**, 9703–9711.
95 A. Lennert and D. M. Guldi, *ChemPhotoChem*, 2019, **3**, 636–644.
96 H. Michaels, I. Benesperi, T. Edvinsson, A. B. Munoz-Garcia, M. Pavone, G. Boschloo and M. Freitag, *Inorganics*, 2018, **6**, 53–70.
97 R. R. Rodrigues, J. M. Lee, N. S. Taylor, H. Cheema, L. Chen, R. C. Fortenberry, J. H. Delcamp and J. W. Jurss, *Dalton Trans.*, 2020, **49**, 343–355.
98 M. Hu, J. Shen, Z. Yu, R.-Z. Liao, G. G. Gurzadyan, X. Yang, A. Hegfeldt, M. Wang and L. Sun, *ACS Appl. Mater. Interfaces*, 2018, **10**, 30409–30416.